University of South-Eastern Norway

www.usn.no

FMH606 Master's Thesis 2022
Process Technology

Safety review and risk study for hydrogen storage

Cathrine Vindenes

Faculty of Technology, Natural sciences and Maritime Sciences
Campus Porsgrunn

University of South-Eastern Norway

www.usn.no

Course: FMH606 Master's Thesis, 2022

Title: Safety review and risk study of hydrogen storage

Number of pages: 71

Keywords: Quantitative risk assessment, hydrogen storage, vapour-cloud explosion, Computational Fluid Dynamics, TNO Multi Energy method.

Student: Cathrine Vindenes

Supervisor: Knut Vågsæther

External partner: -

Summary:

The energy sector is rapidly adjusting towards the green change by cutting emissions and using more renewable energy sources. The interest in hydrogen economy has increased in the last decade due to environmental concerns and the supply of green energy available in the future. QRA reports are prepared to consider and describe the vulnerability of a system, and the consequences and probability of such, to further evaluate any uncertainty and risks. Hydrogen leakage risk is of particular interest due to the wide flammability range, low ignition energy, small molecules, and flame speed. On the other hand, hydrogen has several properties as a safer fuel with being non-toxic, and due to low gravimetric density, the gas it will dissipate quickly into the atmosphere as it is lighter than air.

The presented content of this report is an in-depth literature review of current hydrogen storage options and associated risks, with primary focus of storage leakage. Furthermore, a risk study has been conducted to compare the explosion pressure of a premixed stoichiometric hydrogen-air vapour cloud. The methods applied are the USN CFD FLIC-scheme model and the TNO Multi Energy method, and the methods have been compared with regards to overpressure.

Results from the CFD model show a detonation taking place in each scenario. The confined container with cylinder obstacles is assumed to be the reason for the high blast charge. When applying the TNO ME method the explosion centre was assumed at two different areas for each scenario. The ME-method was assumed to have a blast strength number of 10 due to the level of confinement and high reactivity gas. The comparison shows that the CFD FLIC scheme return significantly higher values for overpressure than ME-method.

Preface

This project has been executed to fulfil the graduation requirements and is part of the last course of the Process Technology masters' program at the University of South-Eastern Norway. The course constitutes of 30 credits, and the presented work was carried out as a part-time study in 2022.

Acknowledgments

I would especially like to thank my supervisor Knut Vågsæther for guiding me through this project. Also, I would like to express appreciation for my degree obtained at University of South-Eastern Norway. Furthermore, I would like to express gratitude to my family and colleagues for supporting me through this period.

Bergen, November 2022

Cathrine Vindenes

Contents

Nomenclature

Abbreviations:

Symbol	Description
2D	Two dimensional
3D	Three dimensional
AIChE	American Institute of Chemical Engineers
CFD	Computational Fluid Dynamics
ESA	Event stream analysis
ESD	Event Sequence Diagram
ETA	Event tree analysis
EPB	Escalation prevention barrier
FAE	Fuel Air Explosion
FLIC	Flux Limited Centred
FTA	Fault Tree Analysis
HAZID	Hazard Identification
HAZOP	Hazard Operability
HE	Hydrogen Economy
HFL	Higher Flammability Limit
HRS	Hydrogen Refuelling Station
HyRAM	Hydrogen Risk Assessment Models
IEA	International Energy Agency
LES	Large Eddy Simulation
LFL	Lower Flammability Limit
LHS	Liquid Hydrogen Storage
LOHCs	Liquid organic hydrogen carriers
MatLAB	Matrix laboratory Software
MC	Monotonized central
ME	Multi Energy
USN	University of South-Eastern Norway
TV	Total Variation
TVD	Total Variation Diminishing
VCE	Vapour Cloud Explosion
QRA	Quantitative Risk Analysis

Latin symbols:

Symbol	Description	
E	Energy	[J]
F	Flux	[-]
k	Turbulent kinetic	[-]
mw	Molecular weight	[g/mol]
p	Pressure	[Pa]
r	Density	[kg/m^3]
R	Gas constant	[J/K*mol]
T	Temperature	[K]
U	Velocity	[m/s]
V	Volume	[m^3]
Q	Heat of combustion	[MJ/m^3]

Greek symbols:

Symbol	Description	Unit
β	Conservation of species variable	[-]
γ	Heat capacity ratio	[-]
ρ	Density	[$kg/m3$]
Δ	Difference	[-]

1 Introduction

1.1 Background

The energy sector is rapidly adjusting towards the green change by cutting emissions and using more renewable energy sources. There has been an increasing interest in the hydrogen economy (HE) in the last decade, and this is primarily due to concerns regarding the energy supply ability and the effect the current energy usage has on the environment. Hydrogen is becoming a viable clean option as a future fuel with both the potential for transportation and storage in larger quantities. (A. Scipioni 2017) Having the possibility of being utilized as a low emission fuel, hydrogen also has a great advantage in the obtained knowledge and existing infrastructure within the wide current usage, such as refineries (for hydrocracking and desulphurization) and agriculture (fertilizer production). (EIA 2016)

For hydrogen to be a competitive dominating fuel in the future, it is important to investigate three major elements in the process such as sustainability, using primarily renewable energy sources, as well as being a cost-effective alternative. When considering the future of hydrogen economy, upscaling the storage ability is crucial. The purpose of larger stationary hydrogen storage facilities is to be able to balance the market with respect to delivery cost when considering changes in supply and demand. This includes being able to store larger quantities of energy for periods with low energy availability.

Assuring safe infrastructure for hydrogen storage is important due to the possible hazards when handling hydrogen considering its physical and combustion properties. The safety parameters for the design system are determined through completing a risk assessment, as well as analysing previous data and research experiments. Although there are clear international safety guidelines prepared, there is no way of knowing if the conducted assessments present the correct risk evaluation of the system, however such an assessment will provide a better understanding for the possible uncertainties in the process. (IEA 2019)

The American Institute of Chemical Engineers (AIChE) defines a Vapour Cloud Explosion (VCE) as "The explosion resulting from the ignition of a cloud of flammable vapor, gas, or mist in which flame speeds accelerate to sufficiently high velocities to produce significant overpressure". (AIChE 2022) Hydrogen is a colourless gas and lighter than air, and a gas-air mixture will only react and ignite through a spark or flame, causing a fire or possibly an explosion. When analysing hydrogen explosions from pre-mixed vapour-gas clouds, occurring due to a leakage, mathematical models are applied to measure the load imposed on the surrounding environment and structures from the explosion. TNO Multi-energy method (Berg 1985) is a simple mathematical model measuring parameters such as the positive overpressure and positive phase duration. More complex models using Computational Fluid Dynamics (CFD) will provide more precise consequence estimates that will help to better understand the mechanism of an explosion.

1.1.1 Hydrogen storage

Hydrogen is an environmentally neutral element, it does not cause any damage, and can be stored in liquid or gaseous form and be used for power, fuel or as feedstock for industry. Hydrogen is produced through chemical reactions as its seldom found in pure form, with methods such as green zero emission hydrogen produced through electrolysis by using electricity from renewable sources to split water into oxygen and hydrogen, or hydrogen produced from hydrocarbons from the oil and gas industry. (Energy 2022) Figure 1.1 below shows an overview of the hydrogen production cycle.

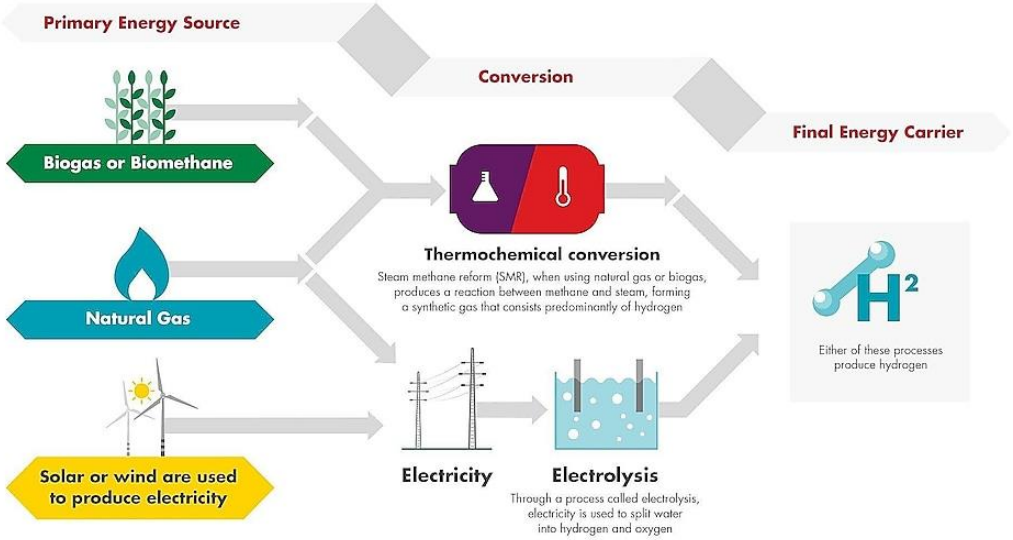

Figure 1.1 Hydrogen production cycle (Shell 2022)

Hydrogen is a very abundant element on the earth as well as in our solar system. Under normal conditions of pressure and temperature (1 atm., 20 ºC) hydrogen appears in a gaseous state and is colourless, odourless, and tasteless. Whilst hydrogen is a non-poisonous gas, it is however a highly flammable gas.

One of the key sections of hydrogen economy (HE) is hydrogen storage and an important enabling element in advancing the technology towards large scale usage. Hydrogen, compared to other fossil fuels, has a low energy density on a volumetric basis requiring increased space demands, but on the other hand a great gravimetric energy density on a mass basis resulting in minimal weight considerations. 1 kg of hydrogen gas occupies over 11 m^3 at room temperature and atmospheric pressure. (J Anderson 2019) Large scale storage opportunity will play a fundamental role in the potential for hydrogen. Considering the expected feasibility of larger storage options with respect to the economic aspect, the density of hydrogen must be increased, which can be done through additional energy input by considering using a low storage temperature and high-pressure tanks or utilizing hydrogen binding materials. (Alcock 2001)

There are two main categories for presenting hydrogen storage technology, physical based and material based, as seen in figure 1.2. Physical based storage includes compressed gaseous hydrogen, cryo compressed hydrogen, and liquid hydrogen. Material-based storage is utilized by physical or chemical sorption; adsorption by storing it on the surface of a material, and absorption by storage it within material. (Global 2022)

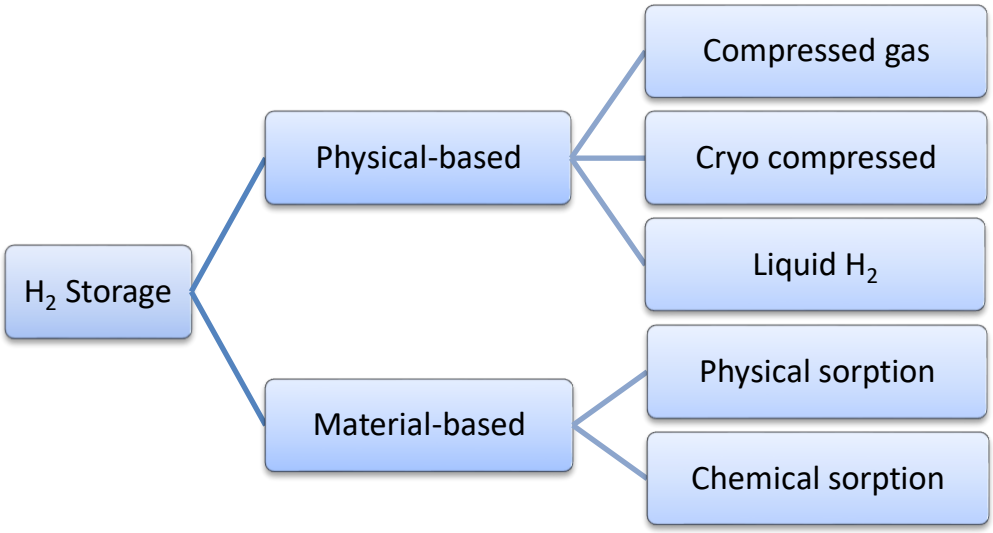

Figure 1.2 Types of hydrogen storage methods (R. Moradi 2019)

1.1.1.1 Physical based storage

Storing compressed hydrogen gas requires storage under high pressure, between 350-700 bar, and this is currently the most established technology for hydrogen storage. The different storage vessels currently utilized include all metal vessel, composite cylinders, partial or fully wrapped vessels with metal- or plastic liner. (T. Smolinka 2021) For physical based storage with compression, the density still only accounts for ¼ of the volumetric density of gasoline. (Energy 2022) Storing gaseous hydrogen in salt caverns has several advantages and is currently used for hydrocarbon refineries. Salt caverns is a flexible, resilient, and safe option but disadvantages with these caverns is possible contamination and geographic scarcity which makes it less viable in some regions. (Engie 2021)

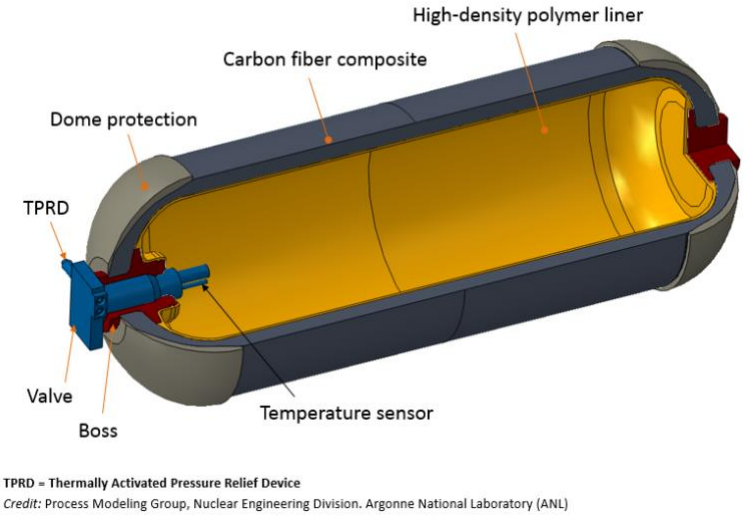

Figure 1.3 Illustration of hydrogen storage tank (ANL 2022)

Liquified hydrogen needs to be cooled to cryogenic temperature (-253.0°C) and storage tanks needs to be insulated to prevent any boil off losses due to liquid hydrogen evaporating during storage (boil off takes place at -252.8°C). (Ghafri 2022) This can occur especially when using smaller storage tanks with high surface area to volume ratio. Liquid hydrogen is often applied when the requirement for high purity is applicable. Cryogenic compressed storage combines the element of compression and cryogenic temperatures, and compared to compressed hydrogen storage, the cryogenic temperature will require lower pressures to be implemented in the storage unit. In addition, this method has shown promising results considering safety level and storage capability with higher density capacity. However, the main challenges include both availability and infrastructure cost. (R. Moradi 2019) Considering the energy demand by using current technology to compress or liquify hydrogen, physical based storage for larger amount of hydrogen is expensive. The different storage methods and conditions variate but it is estimated around 10% of the total energy is used for gas compression storage and around 30% when liquifying. (Energy 2022)

Table 1.1 Properties of hydrogen (Hansen 2019)

Hydrogen in air at atmospheric conditions	
Flammability limits (vol.%) LFL, HFL	4.0, 75.6
Auto-ignition temperature (°C)	560
Cryogenic temperature (°C)	-253.0
Boil off temperature (°C)	-252.8
Maximum laminar burning velocity (m/s)	3.25
Minimum ignition energy (mJ)	0.017
Heat of combustion (MJ/m^3)	3.01
Flammable range in air (%)	4 - 75
Stoichiometric in air (%)	29.5

1.1.1.2 Material based storage

Material based storage is either by adsorption by storing hydrogen molecules on larger surface areas as in the case of porous materials (solid or powder form), or absorption by storing molecules within a material as in the case of hydrides (metal/chemical). Hydride storage combines storage in a reaction between solid and liquid material.

Physical sorption creates a weak bind onto the adsorbent surface through van der Waals forces (vdW) holding the molecules together, chemical bonds are not formed. Throughout the cycle of using physical sorption, one is able to preserve the molecular form of hydrogen and this technique requires lower binding energy than chemical sorption. (Purewal 2010) Metal organic frameworks (MOFs) and porous carbon material has shown promising results as a solutions for storage. (R. Moradi 2019) Sorbents can offer a higher volumetric density to that of physical based compressed hydrogen. (Energy 2022)

Chemical sorption is a chemical reaction between the surface and the absorbate where hydrogen is stored through splitting the atoms to further be absorbed and integrated in a material. Sorbents most famous are metal hydrides where hydrogen is bound in a fine metal hydride powder and deliver more compact storage. In addition, hydrides are suitable for long term storage. (Hereon 2022) There are several advantages with material-based storage such as higher temperatures and lower pressure comparatively to physical storage, and there is greater availability to store larger amount of hydrogen in smaller volumes. Liquid organic hydrogen carriers (LOHCs) are a promising option as the liquid carrier can be reused as its not consumed and managed at ambient conditions.(R. Moradi 2019)

Storing larger amounts of hydrogen is still an obstacle due to high costs and processing time. For hydrogen to become a viable replacement option for the green change, the production of hydrogen must become more efficient, and be executed with a lower production and storage cost, as well as it must be produced from mainly non-fossil fuels. Volumetric density of storage is a continuous problem. In addition, reversibility is an important matter, and moderate operating pressure and temperature. (Gkanas 2020)

1.2 Hydrogen storage risks

Comparatively to other energy systems, hydrogen will also be related to possible risk that could pose a hazardous situation on the surrounding environment and people's safety. A hazard or risk is defined as "a source or a situation with the potential for harm in terms of human injury or ill-health, damage to property, damage to the environment, or a combination of these". (Australia 2022) There are several precautions necessary to be implemented when conduction a risk analysis into such a system. However, it is important to not lose sight of the fact hydrogen has several properties that make it safer than other fuels such as it being non-toxic and when released it will dissipate quickly into the atmosphere as it is lighter than air. (Global 2022)

This report will focus on hydrogen storage leakage. As previously mentioned, hydrogen is a non-poisonous gas but highly flammable, and therefore the risk of hydrogen leakage can cause severe hazardous events where a combustible mixture if formed and lead to an ignition. Leakage in hydrogen storage can produce a mixture that can be flammable or at worst case detonable, either instantaneous (by rupture) or continuous (by example of leak in component). Hydrogen has a low ignition energy compared to fossil fuels and a wide curve area of flammability, and it is therefore at utmost importance to have ensured a safe storage operation by implement leak detecting sensors and provide proper ventilation. Number of risks potential when a leakage occurs:

- Dispersion of hydrogen (followed by ignition),
- Explosion of hydrogen (followed by a jet flame),
- Instant ignition with resultant jet flame.

On a volumetric basis, hydrogen would leak around three times faster than natural gas, due to hydrogen containing the smallest molecule. On the other hand, with a low gravimetric density hydrogen has a higher buoyancy and will dissipate more quickly into the atmosphere. (H. Dagdougui 2018)

In recent years we continue to see instances of industrial accidents from hydrogen storage such as the 2019 Kjørbo incident (Hansen 2019) where there was a fire in a hydrogen station in Sandvika, Norway due to a leak from a high-pressure bearing in a 950-bar tank. The leak is believed to be caused by an incorrectly fitted plug causing a small leak for hours before a sudden failure releasing 1.5-3.0 kg in 3 seconds resulting in a strong explosion. In Santa Clara, California (2019) a hydrogen explosion incident occurred at a refuelling station of gaseous hydrogen where 250 kg of hydrogen was released causing a large explosion with two minor injuries. The cause of the leak was unauthorized maintenance not following set procedures. (Panel 2021) There was also a leakage and explosion in Waukegan, Illinois in 2019. These incidents remind us of the potential risk of blast waves from hydrogen explosions, confined or unconfined, which can cause severe damage to the environment and surroundings of the storage structure. Following these incidents there has been comprehensive review of the safety of the facilities as well as maintenance with similar installations, and the industry sector continues to look for improvements of the opposed risk such as improving control routines and more advanced sensor technology.

1.3 Problem description

The objective of this report is to investigate risks associated with hydrogen storage and perform a risk study of hydrogen storage leakage on a premixed vapour cloud. The project includes the following systematic approach:

- In-depth literature review of available quantitative risk analysis and consequence prediction methods for hydrogen storage. The reviewed material will primarily contain studies on hydrogen leakage.

- Applying an available in-house USN FLIC-scheme model to perform a CFD analysis into a hydrogen storage, presenting a scenario of a 40ft container and simulate a premixed hydrogen vapour cloud explosion. The models used for the explosions are the conservation equations of mass, momentum, and energy, given in equations 1.1 to 1.3.

- Perform a TNO Multi-Energy method case study with the same scenario and variables as CFD and compare results with the results achieved from CFD analysis.

The project topic description of the thesis is given in Appendix A.

$$\frac{\partial \rho}{\mathrm{dt}} + \frac{\partial}{\partial \mathrm{x_i}} \cdot (\rho \mathrm{u_i}) = 0 \tag{1.1}$$

$$\frac{\partial \rho u_i}{\partial \mathrm{t}} + \frac{\partial}{\partial \mathrm{x_j}} \cdot \left(\rho \mathrm{u_j u_i}\right) = -\frac{\partial \mathrm{p}}{\partial \mathrm{x_i}} + \frac{\partial}{\partial \mathrm{x_j}} \left(\mu \frac{\partial u_i}{\partial \mathrm{x_j}}\right) \tag{1.2}$$

$$\frac{\partial \mathrm{E}}{\partial \mathrm{t}} + \frac{\partial}{\partial \mathrm{x_i}} (\mathrm{u_i E}) = -\frac{\partial}{\partial \mathrm{x_i}} (\mathrm{p u_i}) + \frac{\partial}{\partial \mathrm{x_i}} \left(\lambda \frac{\partial \mathrm{T}}{\partial \mathrm{x_i}}\right) \tag{1.3}$$

1.4 Report structure

The thesis is divided into 7 chapters.

- Chapter 2: In-depth literature review of risk prediction methods for hydrogen storage with focus on available literature on hydrogen storage leakage.
- Chapter 3: Models and method. Introduction to dispersion and explosion, presentation of the CFD model and further description of the USN FLIC-scheme.
- Chapter 4: Simulation of gas explosion. This chapter will introduce the initial scenario, including geometry and initial condition, and results obtained from the CFD model.
- Chapter 5: TNO Multi Energy-Method. This chapter will introduce the initial scenario, including assumptions made and initial condition, and results obtained from the TNO ME-method.
- Chapter 6: Discussion of the individual results and comparison of CFD FLIC-scheme along with TNO Multi Energy method.
- Chapter 7: Conclusion of the thesis work.
- References.
- Appendices: Provide additional information and figures that are not given in the report.

2 Review of QRA for hydrogen storage

This chapter will cover an in-depth literature review into available QRA and consequence prediction methods for hydrogen storage. Based on the literature review, several different focus areas were identified:

- Hazard identification
- Consequence analysis
- Frequency analysis

The available literature on these models is presented in the following sections.

2.1 Quantitative Risk Analysis

A QRA (quantitative risk analysis) is a systematic technique that is used to estimate risk and calculate consequences of a hazardous event occurring within and around facilities typically containing and administrating hazardous substances, including hydrogen. The purpose of a QRA study is to understand the total risk of a process, and the analysis should be conducted in such a way so that they can be verified, recreated, and compared independently regardless of technique or person used to perform the analysis. The analysis can help to estimate or predict accidents, fatalities, economic losses, impact on the environment as well as the effect of the assumptions made in a case scenario. The outcome of a QRA can also help set the framework regarding the requirements for the design of a system and implement preventative measures. (Geel 2005)

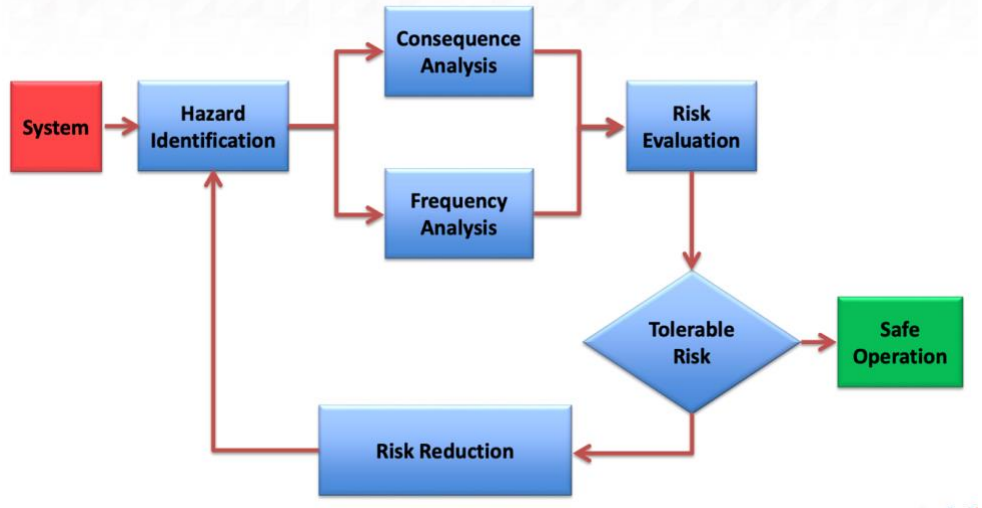

Figure 2.1: QRA Process (J. Dunjo 2017)

When conducting an analysis, it is important to be mindful that the total overview of which events contribute most to the risk is maintained throughout the process, and consider which barriers are critical and most effective, and the precision on the representative risk contours. The risk analysis should therefore use the most expected levels of assumptions and most realistic interpretations of how far one can expect the consequences of the assessed scenarios to extend. After all the risks have been evaluated with possible consequences the tolerable risk will be mapped out from modelling what events will cause death, and after setting the limit for acceptable death rate. (A. Risan 2021) This report will focus on reviewing more recent publications from the last decade.

2.1.1 Overview of literature review

Year	Title	Author	Objective	Method	Highlights
2022	Feasibility Investigation of Several Hydrogen Generation & Storage Methods	Z. Jiang	Quantitative investigation, feasibility study liquid hydrogen, analyse current large scale storage	Review article, HAZID	Advantage: High purity & vol. energy density, no dehydrogenation. Disadvantage: High consumption when liquifying, low temp. required, difficult long term storage, risk of leakage
2019	Hydrogen storage and delivery: Review of the state-of-the-art technologies and risk and reliability analysis	R. Moradi, K. M. Groth	Review main safety challenges hydrogen systems, identify research needs/gaps	Review article	Need more data large scale applications. Lack of optimal layouts. Economic overview difficult.
2014	Accident modelling and safety measure design of a hydrogen station	A. Alshanini A. Ahmad F. Khan	Provides an understanding of the overall failure probability for each barrier	FT model	Total escalation prevention barrier, scarcity of reliability data for hydrogen storage failure events
2022	Numerical investigation of the leakage and explosion scenarios in China's first liquid hydrogen refuelling station	W. Yuan, J. Li, R. Zhang, X. Li, J. Xie, J. Chen	Consequence assessment at hydrogen fuelling station: layout, leakage parameters, local conditions. Low-temperature and explosion hazard.	CFD (FLACS), with added pseudo-source model for two phase hydrogen	Trailer park nearby will worsen explosion. Explosion result in complete destruction control room and endanger people on the adjacent road when leakage diameter $\geq$ 25.4 mm. By increasing wind speed, hazard decreases.
2022	Data requirements for improving the Quantitative Risk Assessment of liquid hydrogen storage systems	C. Correa-Jullian, K. M. Groth	QRA analysis of LH2 storage. Identify, rank, and model risk for relevant scenario and probability data for releases.	Review, FMEA, FTA, ESD	Lack of reliability data for LH_2 limits a QRA. ESD provided. Need for more information on the effect of operational conditions, with respect to likelihood of ignition.
2009	Review methods estimating overpressure and impulse resulting hydrogen explosion	L. Melani, I. Sochet, et al	Estimating the positive overpressures and positive impulses resulting from hydrogen-air explosions	TNO ME method, BST method	Proposed guidelines for choosing TNO ME class number. BST underpredicts effects open area, overpredicts obstructed area. TNO better fit with experimental data, some adaptions.

Year	Title	Author	Objective	Method	Highlights
2007	CFD modelling of accidental hydrogen release from pipelines	H.Wilkening, D.Baraldi	Model accidental release from a small whole in a pipeline, for hydrogen and methane.	CFD (CFD-ACE), LES model	Large amount of hydrogen flammable mixture observed, hydrogen cloud farther from ground than methane due to buoyancy and a higher sonic speed at release
2005	Evaluation of hazards associated with hydrogen storage facilities	F. Rigas, S. Sklavounos	Highlight hazards arising from hydrogen storage, reveal potential accidents, computational estimation of dispersion	ETA, CFD (CFX-5.7) with k-ϵ model	Simulation results show pressurised hydrogen moving upwards. Liquefied hydrogen spills behaves as a heavy gas, more substantial risk for accidental fires and explosions.
2021	Numerical and experimental analysis of jet release and jet flame length for qualitative risk analysis at hydrogen station	B. Park et al.	Dispersion, jet flame, and heat flux were investigated using HyRAM software by considering accidents at hydrogen refuelling stations.	HyRAM (compared experimental data)	HyRAM results more conservative than experimental results. With same pressure, diffusion distance increased as the leak diameter increased.
2020	Leak frequency analysis for hydrogen-based technology using bayesian and frequentist methods	M. Kodoth et al.	Identify trends based on quantitative method, propose a leak frequency rate estimation method.	Time based method	Main results: the leak rate changes according to the time function for the log-normal and Weibull models. Results examined with two other available models.
2009	Analyses to support development of risk-informed separation distances for hydrogen codes and standards.	LaChance et al.	Generate estimates for the total leakage frequency for typical hydrogen gas storage facilities	Leak-hole size method (Bayesian method)	Only generic leak frequencies as some data was not available for H2. Table comparing generic leak to hydrogen leak frequency.
2006	System-analytic Safety Evaluation of the Hydrogen Cycle for Energetic Utilization	A. Rosyid	Perform QRA to evaluate risk and frequency of accidents outcome of hydrogen storage leakage.	Probabilistic safety analysis-: ET & FTA analysis	1% result in explosion, 59% result in fire 40% may have no effect on population Individual risk higher than LPG, societal risk lower, all over lower risk to public.

Hazard Identification
Consequence Analysis
Frequency Analysis

2.1.2 Hazard identification

When starting to plan a risk analysis, a HAZID (Hazard Identification) needs to be conducted to identify potential events that could influence the process. In the HAZID the entire process is analysed, including system, equipment, and operational and maintenance relations. FTA (Fault Tree Analysis) and HAZOP (Hazard and operability study) can used to complete the HAZID. (A. Risan 2021)

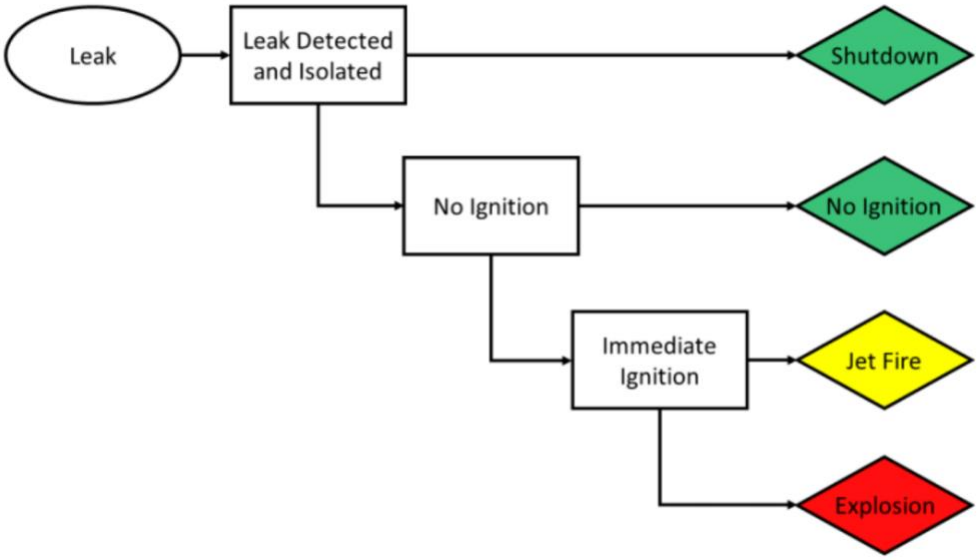

Figure 2.2: Fault Tree Analysis (FTA) leakage model from HyRAM Software. (Sandia 2022)

A review article and feasibility study conducted by Z. Jiang included hazard identification and highlighted advantages and disadvantages when storing liquid hydrogen. A summary from the study is presented in table 2.2. (Jiang 2022)

Table 2.2 Advantages/disadvantages of LHS by (Jiang 2022)

Advantages/disadvantages of LHS	
Advantage	1. High purity 2. No dehydrogenation 3. High volumetric density 4. Relatively good security
Disadvantage	1. High energy consumption when liquifying 2. Require development technology low temp. 3. Difficult long term. storage 4. Risk of leakage

A review conducted by R. Moradi (2019) on the available risk analysis for hydrogen storage draws attention to the lack of available experimental data, especially with regards to the total risk of a complete large scale storage system. As well as the complete economic overview proves to be difficult to obtain, adsorption, chemical or metal hydrides lack optimal layout for large scale. (R. Moradi 2019)

An extensive fault tree (FT) model conducted by (A. Al-shanini 2014) provides an understanding of the overall failure probability for each barrier and includes technical data, and aspects of operational, human and management factors. In addition, the scarcity of reliability data for hydrogen storage failure events is mentioned as a limiting factor, hence information is adopted from natural gas industry as well as other chemical processes. Figure 2.3 below provides the total escalation prevention barrier (EPB) failure FT model conducted in the report. The failure probability for EPB was calculated to be 0.0774 or 7.74%.

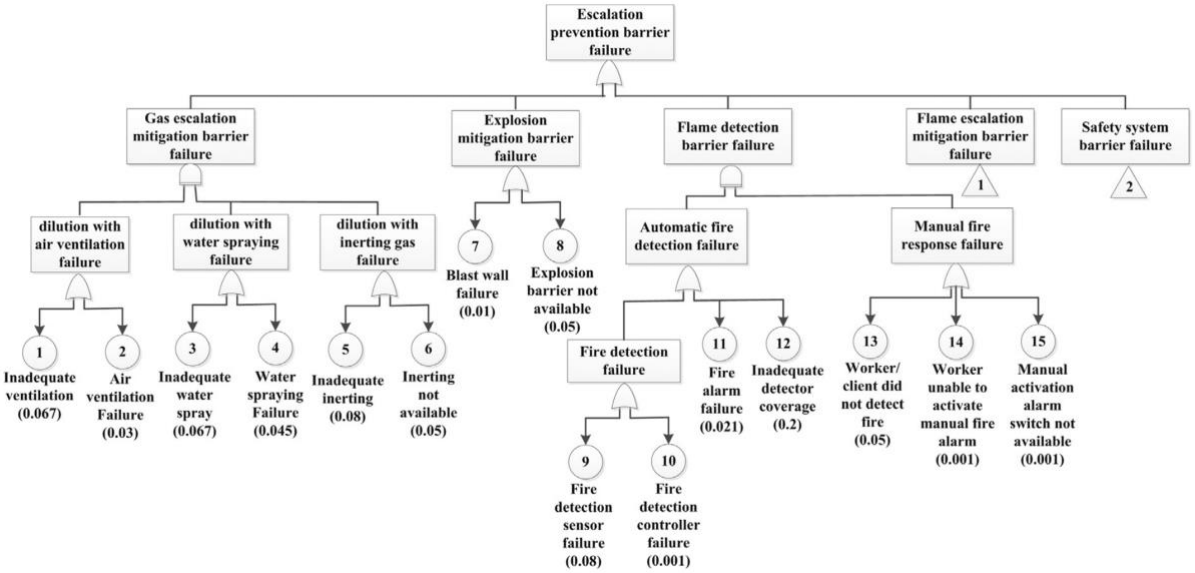

Figure 2.3 EPB failure FT model (A. Al-shanini 2014)

2.1.3 Consequence Analysis

After the HAZID, the identified events are then treated in a consequence analysis which can be done by using tools such as ESA (event stream analysis), ESD (Event Sequence Diagram), bow-tie analysis or similar. In order to predict the outcome of hazards/accidents, the analysis requires previously obtained knowledge of the hazards involved and available information of the material. (Smith 2005)

A consequence assessment on China's first liquid hydrogen refuelling station was conducted by using the commercial CFD tool, FLACS, investigating leakage and explosion. Simulation reveal LH2 released in air has the same behaviour as dense gas. If the leakage diameter exceeded 25.4 mm the explosion will completely destroy control room and endanger people on the adjacent road, and obstacles nearby will intensify explosion. Including local wind in the calculations one could see when wind speed increases, explosion hazard decreases. (W. Yuan 2022)

C. Correa-Jullian sheds light on the lack of reliability data for LH_2 which could hinder necessary safety codes and standards. Investigating a generic LH_2 storage system, QRA analysis tools were used to identify, rank and model leakage risk. Based on the identified failure modes, an ESD was created, illustrated in figure 2.4. The report specifies the need for more information on the effect of operational conditions, with respect to likelihood of ignition. (C. Jullian 2022)

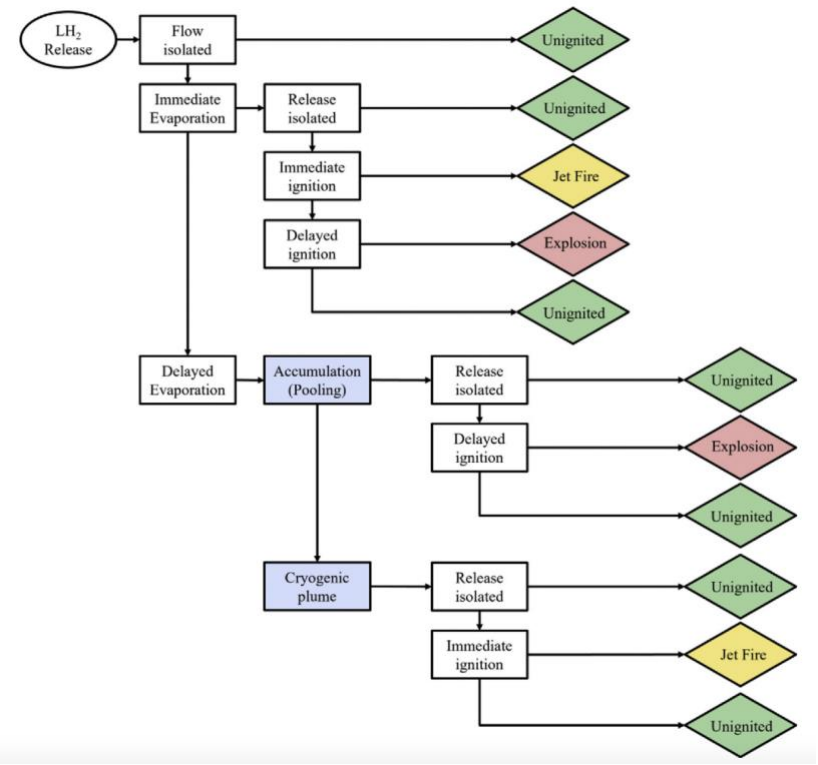

Figure 2.4 Proposed event sequence diagram for LH2 releases. (C. C. Jullian 2021)

L. Melani et al. used the TNO Multi Energy (ME) method and the Baker-Strehlow-Tang (BST) method to estimate positive overpressure and positive impulse. The methods then were compared together with large scale experiments, one scenario presented below in figure 2.5. BST underpredicts effects open area, and overpredicts obstructed area. TNO was a better fit with experimental data with some adaptions, and guidelines for choosing class number for TNO was proposed, presented in table 2.3. The differences seen in overpressure and impulse compared to experimental data is presumed to be due to be the reactiveness of hydrogen, and in addition ignition strength is not a parameter in the BST method. (L. Melani 2007)

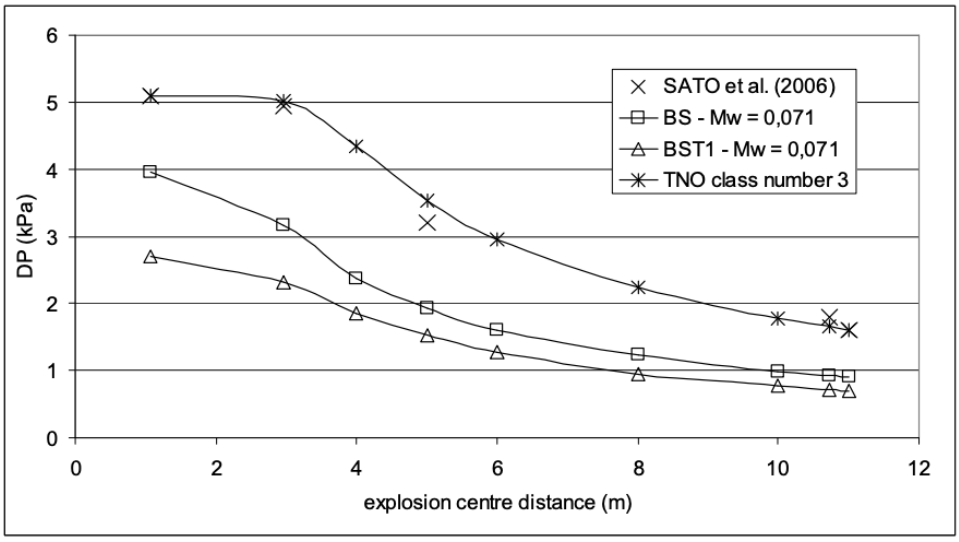

Figure 2.5 Overpressure versus explosion centre distance for experiment in an open area (L. Melani 2007)

Table 2.3 Guidelines for choosing the class number for the TNO Multi-Energy method applied to hydrogen explosion (L. Melani 2007)

High fuel reactivity			
Ignition power	Obstruction	Volume (m^3)	Class number
Low (0 to 150 J)	0 to 1 %	≅ 5 to 2094	3
	1 to 15 %	5 to 300	5 or 6
	4.40 %	≅ 17	7 or 8
High (150 to 5.2 x 10^4 J)	0 %	300	9

A CFD simulation of an accidental release from a pipeline was completed for both hydrogen and methane. LES (Large Eddy Simulation) and k-ϵ model was both implemented but LES produced faster simulation results. As expected, results of a larger total amount of flammable mixture was seen with hydrogen release, and hydrogen cloud was farther from ground than methane due to buoyancy and a higher sonic speed at release. The report concluded with flame acceleration can increase with obstacles present, and ignition is more likely at ground level. (H.Wilkening 2007)

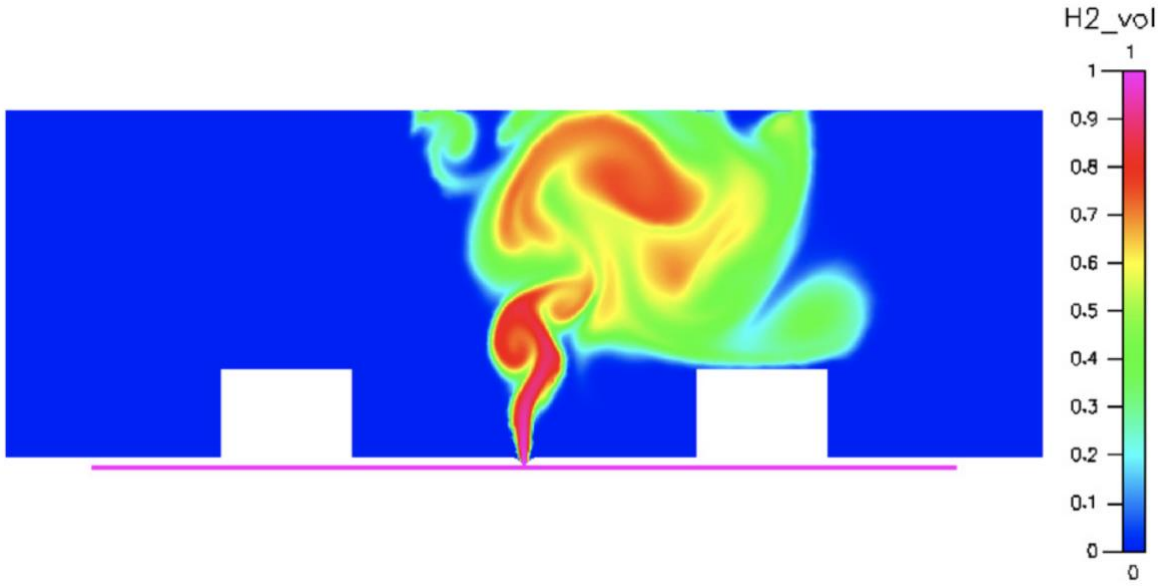

Figure 2.6 Hydrogen volume concentrations after 4 s of high-pressure release from the pipeline and wind at 10 m/s from left to right. (H.Wilkening 2007)

An event tree analysis (ETA) of hydrogen release showed that determination of the lower flammability limit (LFL) distance is of great importance to prevent accidents unless an immediate ignition occurs. Estimating hydrogen dispersion (F. Rigas 2005) used the CFD code CFX-5.7 incorporated with a k-ϵ turbulence model. An extraction of the results demonstrated in Figure 2.7a-b, the vapour cloud dispersion shows pressurised hydrogen moving upwards whilst cryogenic travels in a downwind matter. (F. Rigas 2005)

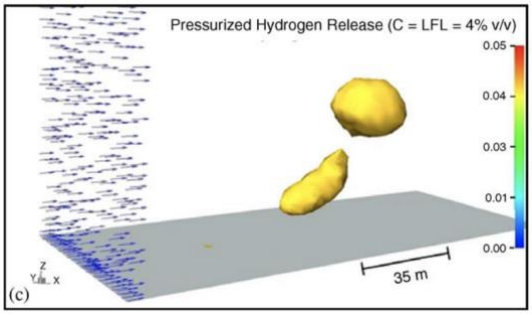

Figure 2.7a Pressurized hydrogen release after 9.6s (F. Rigas 2005)

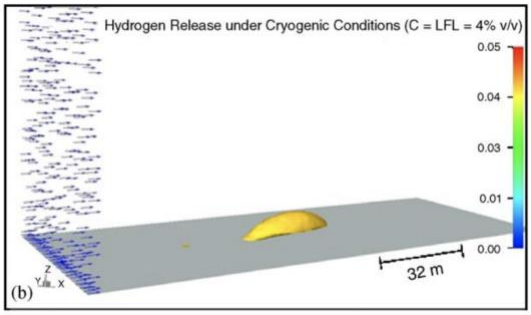

Figure 2.7b Cryogenic hydrogen release after 10s. (F. Rigas 2005)

2.1.4 Frequency Analysis

When calculating the total risk of a system, analysing the likelihood or frequency of an event is of crucial matter. There is generally a good understanding for the consequence research part of an analysis, however being able to understand the likelihood of such an event will help determine the total risk of each individual possible occurrence, and apply ranking systems such as a risk matrix. (K. Shaba 2022) According to (LaChance 2009) there is still a scarcity of available frequency data for usage in QRA on components for hydrogen leakage events, and information on operational data and smaller leakage events unfortunately have not been reported accordingly.

For estimating frequency for hydrogen systems, where obtained data is limited, Bayesian analysis will provide better results than frequentist techniques, by having parameters to describe the distribution of likelihood. Bayesian update gives the opportunity of use newly obtained hydrogen specific data to update prior likelihood estimations. When performing a QRA onto a system, these obtained "priors" can be used to describe "posterior" distribution and decide the risk level. (Bayes 2022)

Bayesian theorem,

$$P(H|D) = \frac{P(H)P(D|H)}{P(D)} \tag{2.1}$$

where $P(H)$ is the probability, $P(D|H)$ is likelihood, $P(H|D)$ is the posterior, and $P(D)$ is the evidence of the obtained data.

Hydrogen Risk Assessment Models (HyRAM) is an established software toolkit for hydrogen systems developed by Sandia National Laboratories in California. HyRAM is applicable for analysing hydrogen leaks by using deterministic and probabilistic models, and the core functionality of HyRAM is QRA, and frequency and probability data. (B. Ehrhart 2022)

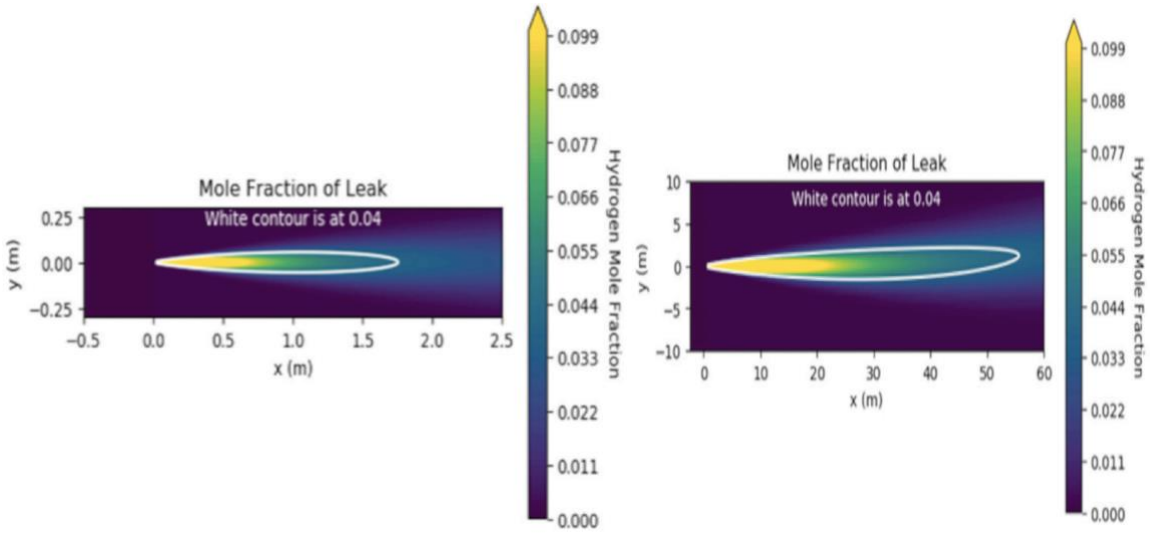

Figure 2.8. Mole fraction distribution at pressure of 82 MPa for leak diameters (left) 0.23 mm and (right) 7.16 mm. (B. Park 2021)

B. Park et al. investigated a jet release with HyRAM using the physics mode, which is used to simulate hydrogen releases, applying data gathered from different accidents in hydrogen refuelling stations. Considering the safety parameters for the hydrogen leakage, the pressure and leak diameter had a considerable influence. The models was performed with the lower flammability limit (LFL), with mole fraction of 0.04. Results showed than independent of pressure, when leak diameter was increased, the diffusion distance also increased. This was in addition applicable when leak diameter was unchanged, when pressure was increased, diffusion increased. (B. Park 2021) Figure 2.7 shows the results from HyRAM of mole fraction distribution at pressure of 82 MPa.

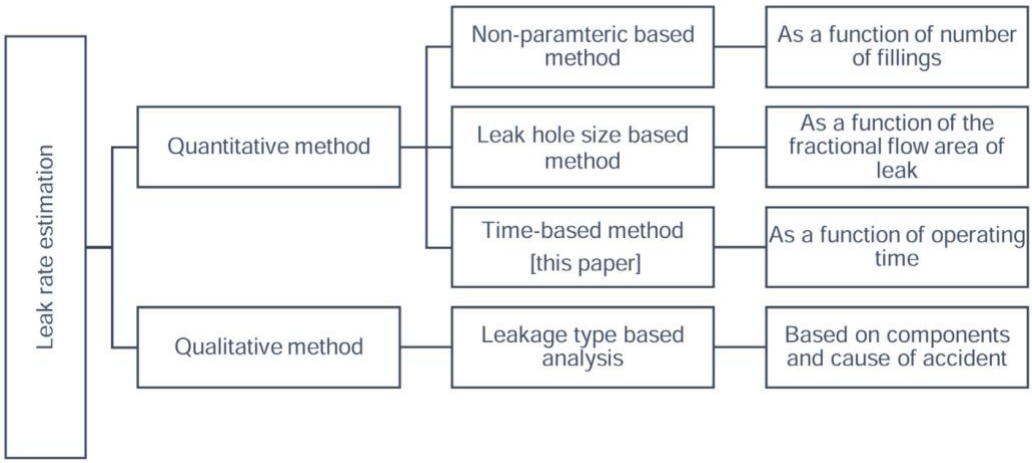

Figure 2.7 Review of methods developed for estimating leak frequency. (M. Kodoth 2020)

A paper by (M. Kodoth et al.) investigated different leak frequency methods. By using previous recorded information from hydrogen refuelling station (HRS) accidents, estimation of leak rate (accident occurrence per unit time per HRS) was proposed using time-based evaluation method, by analysing operational data from HRS and Bayesian update. (M. Kodoth 2020) Time-based methods used are Log-Normal and Weibull, both are continuous probability distribution, however Weibull also accounts for asymmetrical data. Results for leak rate estimation per year are presented in table 2.4. (Frost 2022)

Table 2.4 Leak rate estimation per year (M. Kodoth 2020)

Methods	**Leak rate (per year)**
Log-Normal (time-based) Weibull (time-based)	0.16
Non-parametric Analysis	0.42
Leak-Hole Size Approach	0.20 mm.

A Bayesian frequency model developed by (LaChance 2009) utilizing data from different sources such as the offshore industry, was applied to hydrogen infrastructure to predict the individual leak frequencies for different components. The model contained only generic leak frequencies as some data was not available for hydrogen and was independent of

operating pressure due to type of model and lack of hydrogen specific data. The leakage rates for hydrogen pipes are presented in Table 2.5.

Table 2.5 Results of Bayesian analysis of hydrogen pipes leakage frequencies (LaChance 2009)

Pipe leak size (% of Total flow)	**Generic leak frequencies**	**Hydrogen leak frequencies**
Very small (0.01%)	7.8E-04	8.6E-06
Minor (0.1%)	1.0E-05	4.5E-06
Medium (1%)	4.0E-05	1.7E-06
Major (10%)	5.4E-06	8.9E-07
Rupture (100%)	5.3E-06	5.6E-07

A. Rosyid performed a complete QRA method to evaluate hydrogen production, hydrogen storage, hydrogen filling station, and fuel cells. The report concluded with hydrogen being all over lower risk to the public compared to LPG, by individual risk being higher than LPG, but societal risk lower. The accident outcome frequencies are presented in table 2.6. The frequencies were estimated from a probabilistic safety analysis-analytical approach: combining ET and FTA analysis. The analysis results show 1% results in explosion, 59% results in fire, 40% may have no effect on population. (Rosyid 2006)

Table 2.6 Accident outcome frequencies of the LH2 storage at depot (Rosyid 2006)

Release scenario	**Accident Outcome**	**Conditional Probability**	**Mean**
Instantaneous	Early explosion	0.0072	8.8E-07
	Fireball	0.0287	3.5E-06
	Poor Fire	0.0005	6.3E-08
	Late Explosion	0.0000	2.8E-10
	Flash Fire	0.0000	1.1E-09
Continuous	Jet Fire	0.4801	5.9E-05
	Pool Fire	0.0768	9.4E-06
	Late Explosion	0.0017	2.1E-07
	Flash Fire	0.0069	8.5E-07
No effect		0,3957	4.9E-05
Overall		0,9976	1.2E-04

3 Models and methods

This chapter will include an introduction to hydrogen dispersion and explosions. In addition, introduce the computational model used to simulate a vapour cloud explosion.

3.1 Dispersion and explosion

A hydrogen vapour cloud dispersion occurs through the cloud interacting with air and being transported and diluted by wind in the atmosphere. Dispersion at stationary state is restricted within the atmospheric mixed layer, and there is dispersion due to wind and air fluctuating as the result of the presence of eddies. Existing models today can predict the described dispersion giving an output of a concentration in the mixed layer as a function of time, and will be able to predict the total amount of material existing between the upper and lower flammability limit. (C. van den Bosch 2005) Compared to methane and propane, gaseous hydrogen when released is found to be more diffusive and therefore will disperse more swiftly into the environment, disregarding cryogenic hydrogen as the density concentration of the vapour cloud can have higher density than the air. (Alcock 2001)

The minimum ignition energy for hydrogen is far lower than for other fuels such as methane, propane, and gasoline, where for hydrogen it is 0.02MJ compared to 0.24MJ for gasoline. In addition, hydrogen has substantially wider flammability limits comparatively to other combustibles, with a lower flammability limit (LFL) and upper flammability limit (UFL) ranging from 4 to 75 vol% in air respectively. Figure 3.1 shows minimum ignition value and flammability limits for hydrogen and methane. Considering the risk, the flammable limits is considered a disadvantage, however hydrogen is less likely to have flammable mixtures occur than gasoline and propane, since the LFL is higher for hydrogen than the mentioned fuels (1, 2.1 vol% for gasoline and propane respectively).

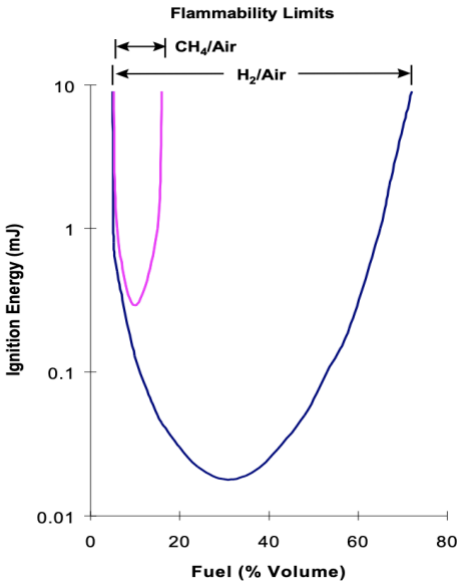

Figure 3.1 Minimum ignition energies and flammability limits for H_2 and CH_4 (Alcock 2001)

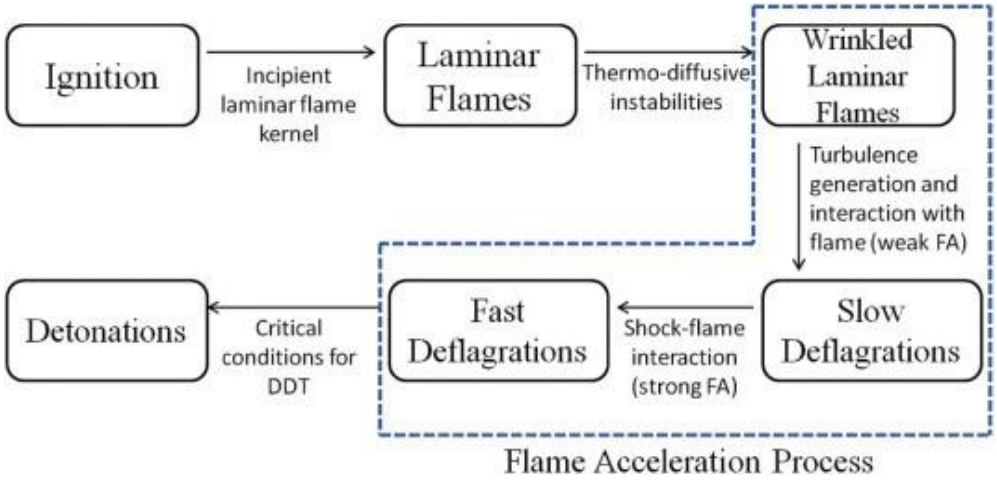

Figure 3.2: Transition from ignition to detonation (Karanam 2021)

Vapour cloud explosion (VCE) is created by an accidental release of a substance, following a dispersion phase where fuels mixes with air and forms a vapour fuel-air cloud prior to ignition. In a VCE the flame acceleration goes to high enough velocities to produce significant overpressure. (C. van den Bosch 2005) The vapour cloud must be with the flammable range limits, as the ignition source set of an explosion. A vapour cloud is classified into different regions; one region between the flammability limits, a region at the point of release with rich fuel content, and a region near the cloud edge with a leaner fuel content. (S. Hanna 1987)

Deflagrations have flame velocity at subsonic speed (below speed of sound) whereas for detonation the velocities are at supersonic speeds, and the detonation will generate higher pressure that will cause larger destruction. The main propagation mechanism for deflagration: Flame front moving towards a gas mixture, and the chemical combustion occurs through diffusion of heat and mass. The main propagation mechanism for detonations: Detonation is a coupled shock and flame front structure. A powerful pressure wave, where the chemical combustion is initiated by shock waves causing compressed heat. A detonation is described to be worst case scenario for accidents containing hydrogen, and the flame range for detonations span from 11-59 vol% compared to the flammability range of 4-75 vol%. There are several factors that needs to be accounted for when estimating the severeness of a hydrogen explosion such as the composition ratio of the hydrogen-air mixture, whether the mixture is uniform or non-uniform, as well as accounting for the presence of congestion/obstacles in the field and confinement around the mixture such as walls or ceiling. (Tretsiakova-McNally 2022)

The effect blast pressure has on structure and the human body can be severe. Around 0.4 bar is considered a dangerous distance with around 50% deathrate, and most building will collapse. For a lower value such as 0.1 bar overpressure can still be dangerous with the likelihood of damaged structure (windows, doors) as well as be harmful to humans due to flying objects. (Zipf 2022)

3.2 CFD model

The simulations in this report are performed by using an in-house CFD code from the University of South-eastern Norway (USN) for explosions to study important effects such as overpressure. These simulations are performed in the programming and computing platform MATLAB version R2022a (Mathworks 2022)

3.2.1 Introduction

Computational Fluid Dynamics (CFD) modelling is a process used for numerical analysis and mathematical modelling of a fluid flow phenomenon, heat transfer and/or chemical reactions. CFD allows one to solve comprehensive problems in early stages of a project that will allow more data availability for decision making, which could save both money and time by obtaining information that is normally obtained by experiments. On the other hand, the results from a simulation must be validated and verified as it cannot be trusted to the same extent as an experiment. A simulated section is set by a control volume, where one defines mesh/cell sizes to be able to extract relevant information like pressure and velocity. By defining boundary conditions such as object surfaces, the simulation can perform calculation in both free stream and with interacting fluids. (H. Versteeg 2007)

In modelling of fluid flow, turbulence in one of the most challenging aspects to model. Many methods have been presented, although there is no general model that would suit every flow scenario. Popular methods applied are the RANS-method and LES-method (Reynolds Average Navier-Stokes and Large Eddy Simulation). These method model sub-mesh solving averaged equations, and turbulence model will account for small scale effects. (Nichols 2003)

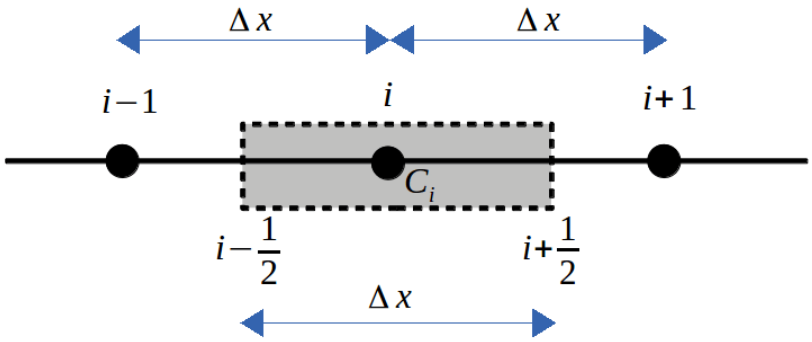

Figure 3.3: Principle of a control volume Ci with uniform discrete nodes. (Gunawan 2018)

Characterizing the flow field is done by applying governing equations for a Newtonian fluid. A Newtonian fluid is a fluid where viscosity is constant, meaning viscous stress is arising linearly correlated with local strain rate. Simplified versions of the conservation equations of mass, momentum, and energy (described by the continuity equation, the Navier-Stokes equation, and total energy equation) are used as basic models and is shown in equation 3.1-3.3.

$$\frac{\partial \rho}{\mathrm{dt}} + \frac{\partial}{\partial \mathrm{x_i}} \cdot (\rho \mathrm{u_i}) = 0 \tag{3.1}$$

$$\frac{\partial \rho u_i}{\partial \mathrm{t}} + \frac{\partial}{\partial \mathrm{x_j}} \cdot \left(\rho \mathrm{u_j u_i}\right) = -\frac{\partial \mathrm{p}}{\partial \mathrm{x_i}} + \frac{\partial}{\partial \mathrm{x_j}} \left(\mu \frac{\partial u_i}{\partial \mathrm{x_j}}\right) \tag{3.2}$$

$$\frac{\partial \mathrm{E}}{\partial \mathrm{t}} + \frac{\partial}{\partial \mathrm{x_i}} (\mathrm{u_i E}) = -\frac{\partial}{\partial \mathrm{x_i}} (\mathrm{p u_i}) + \frac{\partial}{\partial \mathrm{x_i}} \left(\lambda \frac{\partial \mathrm{T}}{\partial \mathrm{x_i}}\right) \tag{3.3}$$

3.2.2 FLIC Scheme

A Total Variation Diminishing (TVD) scheme is used to solve hyperbolic partial differential equations and are often applied in computational fluid dynamics. The transient term and the convective term of conservation equations are hyperbolic, including the pressure forces. The TVD method is a subclass method of the Total Variation Stable (TVS) method, and states that the Total Variation (TV) does not increase with time. (Toro 2009)

The mathematical definition of TVD schemes per (Toro 2009),

$$TV(u^{n+1}) \leq TV(u^n) \tag{3.4}$$

which follows the consequence of the above definition leading to,

$$TV(u^n) \leq TV(u^{n-1}) \ldots \leq TV(u^0) \tag{3.5}$$

where (u^0) is data at time = 0.

The FLIC (Flux LImited Centred) scheme, (Toro 2009), is a second order TVD scheme that has been extended from the FORCE scheme. The FLIC scheme combines the FORCE first order centred scheme with the second order Richmyer version of Lax-Wendroff scheme. (Toro 2009)

First order Lax–Friedrichs scheme:

$$F^{LF}_{i+\frac{1}{2}} = \frac{1}{2}[F(U_i) + F(U_{i+1})] + \frac{1}{2}\frac{\Delta x}{\Delta t}[(U_i) - (U_{i+1})] \tag{3.6}$$

Second order Richtmyer scheme:

$$U^{RI}_{i+\frac{1}{2}} = \frac{1}{2}[(U_i) + (U_{i+1})] + \frac{1}{2}\frac{\Delta t}{\Delta x}[F(U_i) - F(U_{i+1})] \tag{3.7}$$

$$F^{RI}_{i+\frac{1}{2}} = F\left(U^{RI}_{i+\frac{1}{2}}\right) \tag{3.8}$$

where U is the vector for conserved variables and F is the flux vector.

The First Order Centred (force) scheme:

$$F_{i+\frac{1}{2}}^{force} = \frac{1}{2}\left(F_{i+\frac{1}{2}}^{LF} + F_{i+\frac{1}{2}}^{RI}\right) \tag{3.9}$$

General approach of flux limited scheme combines a low order flux with a high order flux:

$$F_{i+\frac{1}{2}} = F_{i+\frac{1}{2}}^{LO} + \phi_{i+\frac{1}{2}}\left[F_{i+\frac{1}{2}}^{HI} - F_{i+\frac{1}{2}}^{LO}\right] \tag{3.10}$$

where $\phi_{i+\frac{1}{2}}$ is the flux limiter.
The FLIC scheme constructed with the fluxes for the FORCE and Richtmyer schemes:

$$F_{i+\frac{1}{2}}^{LO} = F_{i+\frac{1}{2}}^{force}\ ; \qquad F_{i+\frac{1}{2}}^{HI} = F_{i+\frac{1}{2}}^{RI} \tag{3.11}$$

resulting in the full FLIC scheme:

$$F_{i+\frac{1}{2}}^{FLIC} = F_{i+\frac{1}{2}}^{force} + \phi_{i+\frac{1}{2}}\left[F_{i+\frac{1}{2}}^{RI} - F_{i+\frac{1}{2}}^{force}\right] \tag{3.12}$$

FLIC is an explicit solver which addresses time step by time step, and gives a robust, quick, and stable solver. Flux limiters are used to approach flux occurring by the interphase to avoid the oscillations occurring due to shocks or discontinuities. A MC (monotonized central) limiter is applied in this scheme simulation, which is a symmetric limiter ensuring that the limiting actions opposed on the system operates in the same way for backward and forward gradients. The MC-limiter operates somewhere between the 1st and 2nd order scheme. When rapid changes occur, such as shocks, the 1st order flux will be applied as any higher order will produce numerically unstable solutions. Meanwhile the 2nd order flux limiter will operate well in smoother areas of the explosion curve.

Turbulence model applied in the FLIC-scheme is based upon the turbulent kinetic energy (k) equation. The conservation equation describes the production, dissipation, and transport of turbulence, through turbulent viscosity for turbulent stresses, and the rate of change of a fluid particle. The conservation equation of species is a variable (β) set between 0 and 1, where 0 is reactants and 1 is products. (Vågsæther 2010)

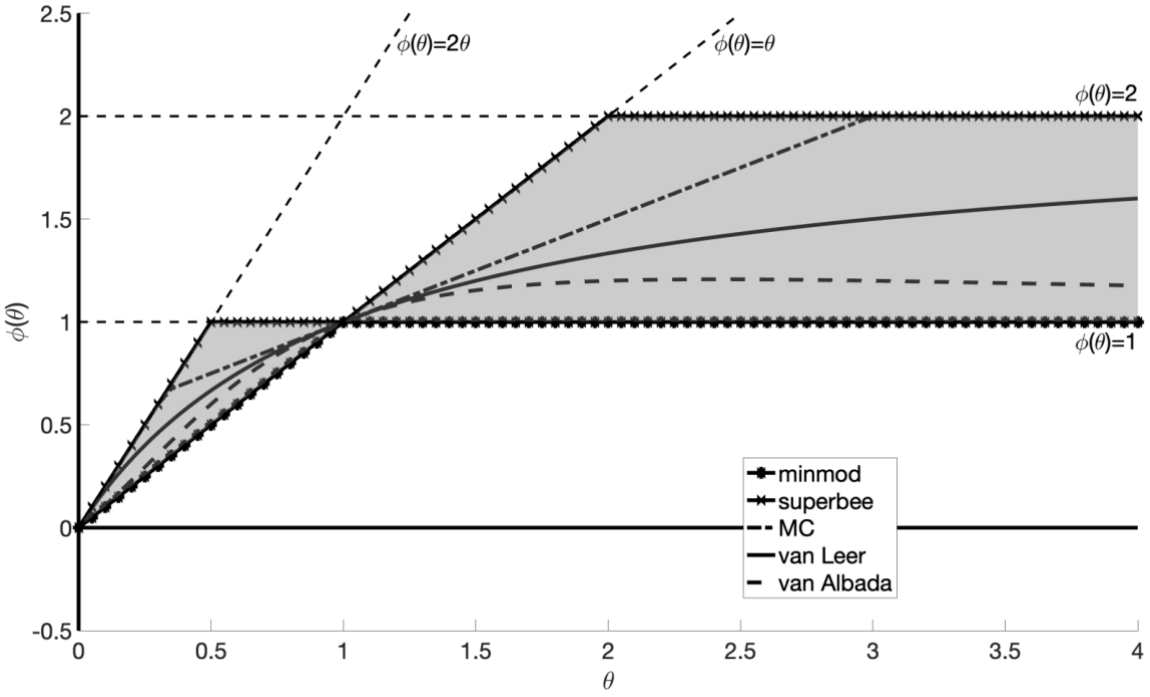

Figure 3.4: The Sweby's diagram (shaded region) and several limiter functions. (Zeng 2022)

The shaded region of figure 3.1 is the TVD region for the Euler equation. In this region, if the limiter function lies within the shaded region, then the scheme will be a 2nd order TVD scheme. In higher order schemes it is common to see many oscillations present, which is not acceptable for any solution. By increasing number of cells for first order scheme, the processing time will increase rapidly, and it not a good alternative. In the smooth regions the first order limiter will give a diffusive result, even with high number of cells. While the second order limited will provide very accurate results without having to increase the number of cells. θ is the ratio of change between neighbouring cells, if $\theta = 1$ the solution is a straight line, uphill or downhill, and the second order scheme will apply. When $\theta = 0$ there is a shock or instability present in form of a sharp hill or a valley, and here first order scheme will apply.

4 Simulation of gas explosion

This chapter will introduce the initial scenario, geometry, and results from CFD model.

4.1 Geometry and set-up

The yellow book defines a vapour cloud explosion as “the explosion resulting from an ignition of a premixed cloud of flammable vapour, gas or spray with air, in which flames accelerate to sufficiently high velocities to produce significant overpressure”. (C. van den Bosch 2005) The initial scenario of the simulation is a premixed fuel-air vapour cloud, where hydrogen is released and dispersed with air to forms a combustible stoichiometric mixture. An explosive charge, a spark, initializes the explosion in the vapour cloud.

The CFD FLIC-scheme presented in chapter 3 in applied in this simulation, and the scripts that has been set up are for this report is ‘geometry.m’ for specifying the geometry and ‘IC.m’ for initial conditions, mesh, and other controlling variables. The total algorithm flowchart for the USN FLIC-scheme is available in Appendix B. (Vågsæther 2010)

The geometry set-up for the simulation is a 40ft ISO container (12x2.6x2.5m) with 9 cylinders containing hydrogen, each with a radius of 0.3m. The geometry of the hydrogen container is presented below in figure 4.1a-b. The scripts for initial conditions (IC.m) and geometry (geometry.m) are given in appendix C and D respectively.

List of simulation specification executed for script for geometry and initial condition:

- Setting the mesh size by setting number of cells in x, y and z-directions.
- Inserting initial field variable values and conditions.
- Insert geometry
- Patch in the shape of the dispersed vapour cloud where the reactive stoichiometric cloud is.
- Patching in an ignition point.
- Specifying the location of the different pressure sensors

Geometry sketch for container including cylinders:

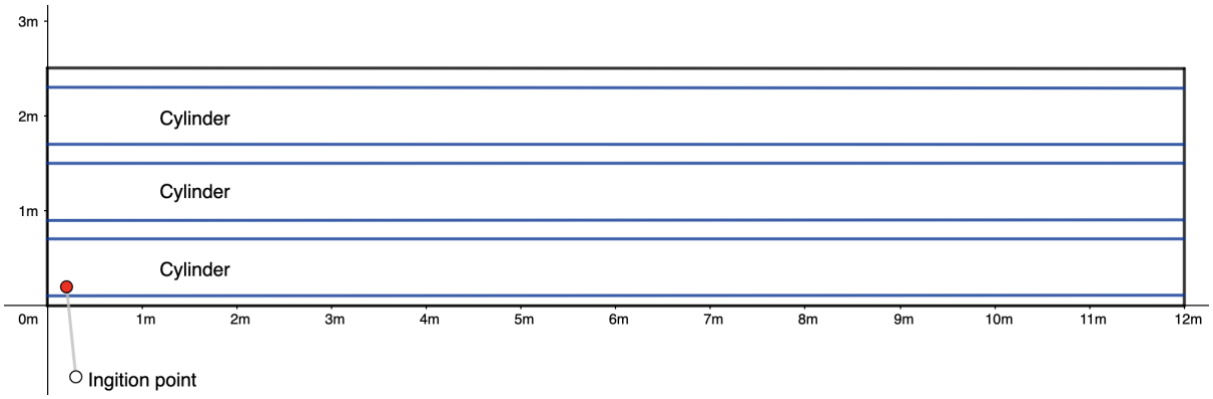

Figure 4.1a 2D Sketch of container geometry side

The geometry measurements for the container and hydrogen cylinders:

- Volume of container: 78m^3.
- Total volume (9) cylinders: 30.5m^3.
- Total available volume (free space) in container: 47.5m^3.

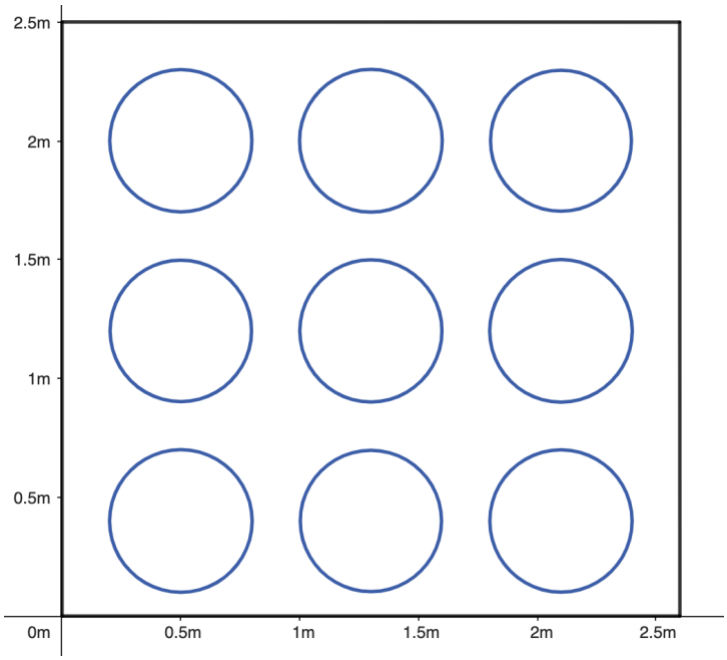

Figure 4.1b 2D Sketch of container geometry front

The total simulated domain consists of following number of cells: (x,y,z) is (340, 125, 80) cells respectively in each direction for the first scenario (1kg). As a result, the total number of cells for the mesh is 3,400,000 cells. The mesh used for this simulation is a uniform homogenous cubic mesh, equal in all directions. Each cell has the size of 0.1m. Having smaller cell size would cause simulation time to increase tremendously, and 0.1m in considered sufficient in the present case study performed in this report. To achieve detailed information regarding the cylinders, the mesh is too course, but however it will be sufficient for the given scenario presented as the focus will be on the vapour cloud explosion and the resulting information obtained outside the container. In addition, it is expected that there possibly could be produced excessive turbulence due to the large mesh cells size applied, which could cause an overestimation of the flame acceleration. (Vågsæther 2010)

The dispersed vapour cloud of the simulation is assumed to have the shape of a crescent rectangle starting at the back of the container and rising out into the air. The mixture is assumed to be at stoichiometric conditions (30% hydrogen), at atmospheric pressure (1bar) and 293 K. In addition, it is assumed the mixture is of uniform composition, with the same composition throughout the area of the cloud.

This report will analyse leakage of 1kg, 2kg and 3kg hydrogen. Vapor density of hydrogen and air at NTP (normal pressure and temperature), 20ºC and 1 atm, is r_{h2} = 0.083 kg/m3 and r_{air} = 1.2 kg/m3 respectively. The specific volume of a gas to express the volume amount per mass unit is the inverse of the density, for hydrogen gas it is estimated to be around $V_{h2,NTP}$ = 12m^3/kg. For stoichiometric mixture of a hydrogen-air vapour cloud at atmospheric conditions, the cloud will consist of approximately 30% hydrogen to 70% air. The total energy in the cloud is constant. Using the ideal gas law to calculate the density of hydrogen at NTP:

$$r_{h2} = \frac{P*mw}{R*T} = \frac{101e^3*2.016e^{-3}}{8.314*293} = 0.083\frac{kg}{m3} \quad (4.1)$$

Where r, mw, P, R and T is the density, molecular weight, pressure, the universal gas constant, and temperature respectively.

Table 4.1 Initial conditions used for the USN FLIC code

Parameter	**Notation**	**Value**	**Unit**
Initial pressure	P_0	$1*10^{-5}$	Pa
Initial temperature	T_0	293	K
Molecular weight air	mw_{air}	$29*10^3$	kg/kmol
Molecular weight H_2	mw_{h2}	$2*10^3$	kg/kmol
Universal gas constant	R	8.314	kJ/kmol*K
Heat of Combustion	Q	3.5	MJ/m^3
Heat capacity ratio	g_1, ga_{unburn}, ga_{burn}, ga_{air}	1.4	-

The calculations used in the simulation uses the conditions of ideal gas law. By doing so, the heat capacity (γ) is constant for all variables in the calculations, as the ideal gas law is applied to model the internal energy. The model is assuming stoichiometric conditions for the vapour cloud, and the reaction will have a high reaction temperature (compared to other fuel mixtures). Therefore it is assumed reasonable with constant heat capacity as the model is not handling the dependent temperature for each gas. (Vågsæther 2010) The ignition spark is set at the end wall at 0.15 meters height, this is simulated by a high pressure and temperature region. The initial conditions are presented in Table 4.1.

The presented released amount of hydrogen simulated is 1kg, 2kg and 3 kg. The computer capability with given mesh size of 0.1m was tested with different free field explosions (only gas present). Originally, the set-up was planned with higher amounts of leakage (1kg, 10kg, 20kg), but was concluded to be out of reach with respect to data capability and computing timeline. The presented results had a computational time between 12-20 hours per scenario.

4.2 Modelling results

4.2.1 Leakage of 1 kg

- Volume of cloud for 1kg release: $V_{cloud} = 40m^3$.
- Geometry of cloud extracted from MatLAB:

```
f(1:120,50:76,1:25)=1;      %Gas present, shape of cloud
r(1:120,50:76,1:25)=0.97;   %Cloud density
```

- Position of pressure sensors extracted from MatLAB:

```
% Set pressure sensor positions
XS=[121,121,121,121,131,141,170,220,230];
YS=[63,53,43,33,63,63,63,63,63];
ZS=[1,1,1,1,1,1,1,12,27];
```

Table 4.2 Sensor overpressure values from CFD model in kPa.

Sensor (no)	1	2	3	4	5	6	7	8	9
Overpressure (kPa)	2120	1540	265	232	2320	2100	516	200	50

The results are presented in Figure 4.2a-b. The results were split up into two separate plots to show the explosion more clearly for two different direction, x-axis and y-axis. Figure 4.2a represents the values going parallel to the contained in the x-direction, and figure 4.2b shows the values obtained perpendicular/sideways out from the container. Each subchapter will be presented in similar set-up with two specific graphs where Figure “a” will present sensors in the x-axis, and figure “b” will present the y-axis values as described.

The graphs show a detonation taking place in each scenario. The confined container with cylinder obstacles is assumed to be the reason for the high blast charge, together with the heigh reactivity and flame speed of hydrogen gas.

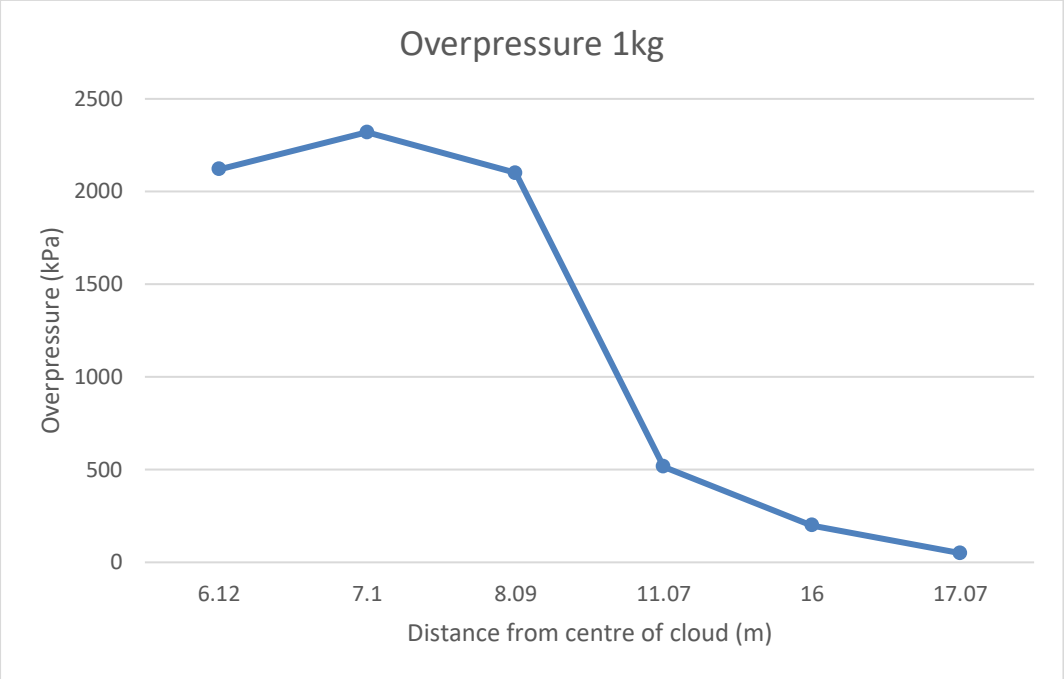

Figure 4.2a Overpressure vs. distance from centre (along x-axis towards post container).

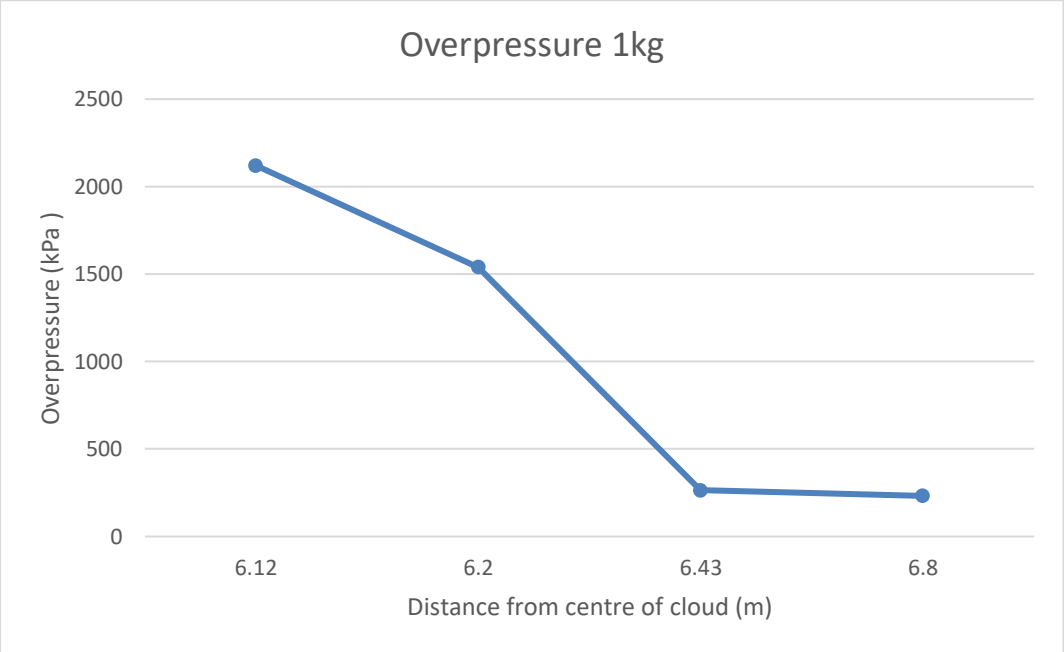

Figure 4.2b Overpressure vs. distance from centre (along y-axis on the right-hand side of container).

4.2.2 Leakage of 2 kg

- Volume of vapour cloud for 10kg hydrogen release: $V_{cloud} = 80m^3$.

- Geometry of cloud extracted from MatLAB:

```
f(1:120,50:76,1:25)=1;      %Gas present, shape of cloud
r(1:120,50:76,1:25)=0.97;   %Cloud density

% add one kg of H2
f(121:160,50:76,13:52)=1;
r(121:160,50:76,13:52)=0.97;
```

- Position of pressure sensors:

```
% Set pressure sensor positions
XS=[121,121,121,121,121,121,141,190,260,270];
YS=[63,53,43,33,23,13,63,63,63,63];
ZS=[1,1,1,1,1,1,1,1,12,27];
```

Table 4.3 Sensor overpressure values from CFD model in kPa.

Sensor (no)	1	2	3	4	5	6	7	8	9	10
Overpressure (kPa)	2120	1550	2860	2670	2060	1570	2400	410	182	57

Figure 4.3a represents the values going parallel to the contained in the x-direction, and figure 4.3b shows the values obtained across and sideways out from the container.

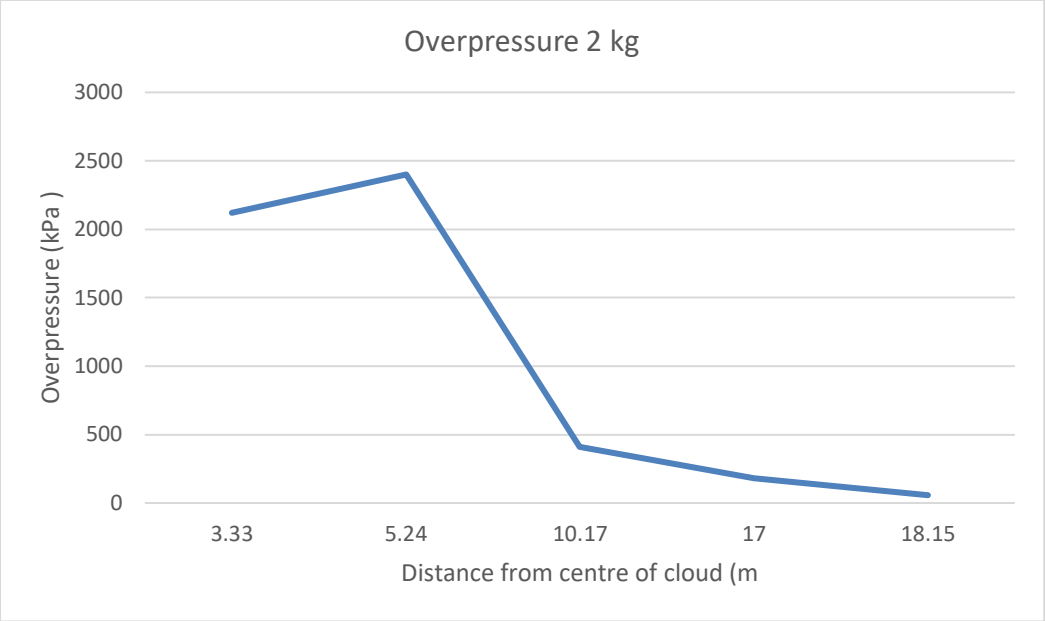

Figure 4.3a Overpressure vs. distance from centre (along x-axis towards post container).

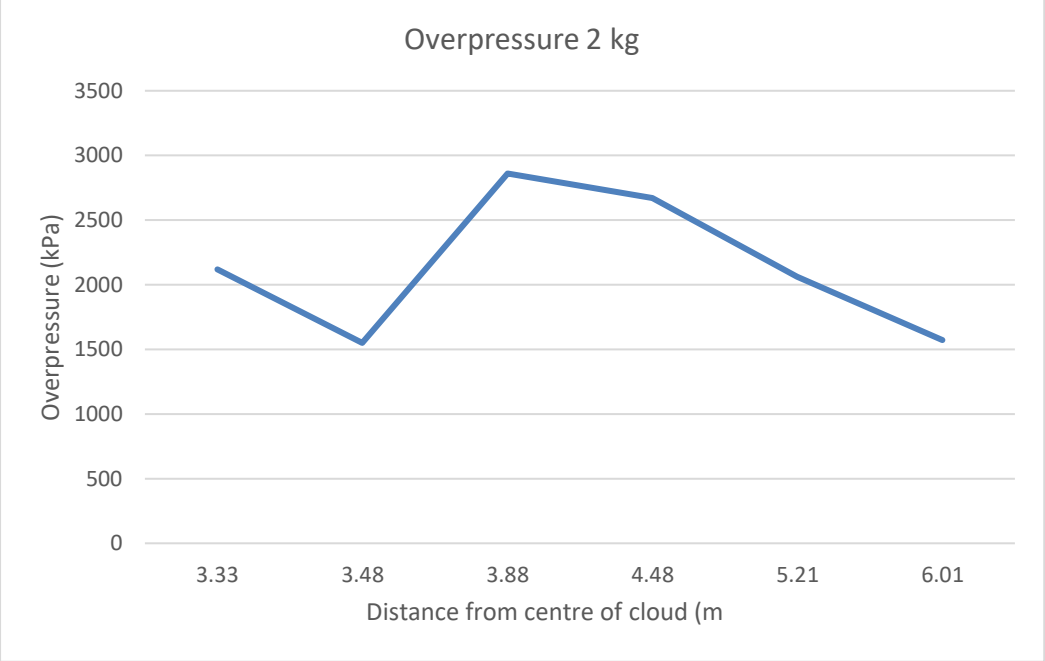

Figure 4.3b Overpressure vs. distance from centre (along y-axis on the right-hand side of container).

4.2.3 Leakage of 3 kg

- Volume of vapour cloud for 10kg hydrogen release: $V_{cloud} = 120m^3$.
- Geometry cloud extracted from MatLAB:

```
f(1:120,50:76,1:25)=1;      %Gas present, shape of cloud
r(1:120,50:76,1:25)=0.97;   %Cloud density

% add one kg of H2
f(121:160,50:76,13:52)=1;
r(121:160,50:76,13:52)=0.97;

% add one kg of H2
f(161:200,50:76,33:72)=1;
r(161:200,50:76,33:72)=0.97;
```

- Position of pressure sensors:

```
% Set pressure sensor positions
XS=[141,141,141,141,141,141,161,210,300,310];
YS=[63,53,43,33,23,13,63,63,63,63];
ZS=[1,1,1,1,1,1,1,1,12,27];
```

Table 4.4 Sensor overpressure values from CFD model in kPa.

Sensor (no)	1	2	3	4	5	6	7	8	9	10
Overpressure (Pa)	2370	1050	3	490	326	222	1100	236	230	68

Figure 4.4a represents the values going parallel to the contained in the x-direction, and figure 4.4b shows the values obtained across and sideways out from the container.

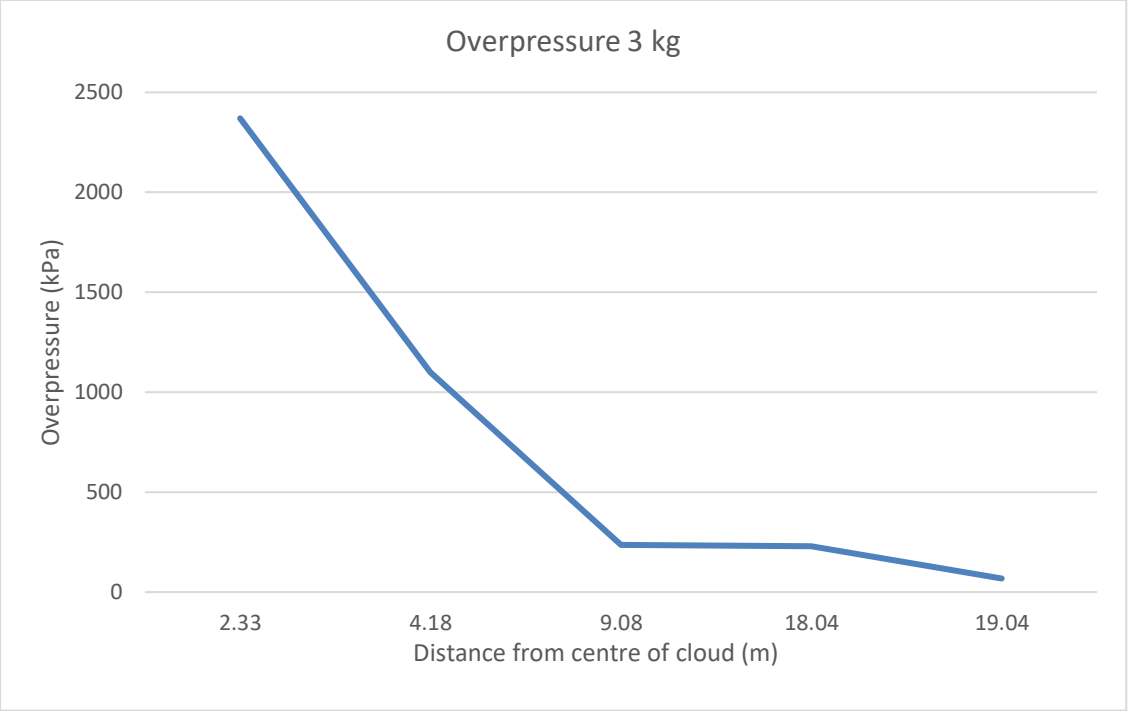

Figure 4.4a Overpressure vs. distance from centre (along x-axis towards post container).

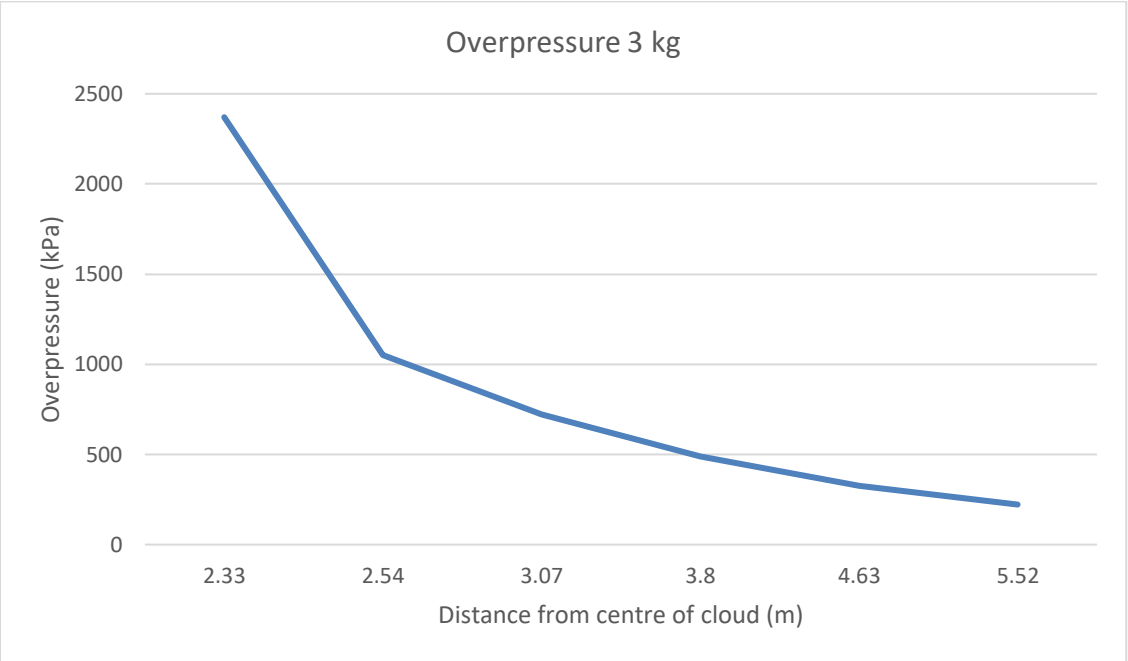

Figure 4.4b Overpressure vs. distance from centre (along y-axis on the right-hand side of container).

5 Multi Energy method

This chapter will include an introduction to the TNO Multi Energy Method and further use the ME-method for a case study for a hydrogen-air vapour cloud explosion.

5.1 The multi energy method

The TNO multi energy method proposed by Van der Berg (1985) is a widely used method for evaluating vapour cloud explosions and is a simple method for vapour cloud explosion blast modelling. The model applies a "blast curve" method and was specifically developed to simulate vapour cloud explosions. Applying the principle of idealized gas explosion, the method evaluates the possible blast potential and considers important factors of the surrounding environment such as blast obstacles, ignition source and spatial density. The method examines the surrounding environment of a gas explosion and uses the boundary conditions given in the scenario's combustion process. It measures the hazard coming from explosions from how the vapour cloud disperses in the surrounding environment, and sub-explosions occurring within the gas vapour cloud. (Berg 1985)

ME-method uses two parameters to describe the explosions strength given by the blast curve number and the mass amount for the explosive fuel. The energy of explosion depends highly on the level of congestion and depends less on the fuel in the vapour cloud. Highly congested structures will give higher overpressure. Hydrogen being a flammable gas with high laminar burning velocity, will also result in higher overpressure. The flow diagram for application of the ME-method is presented in Appendix F: TNO Multi Energy Flow Diagram.

There are some limitations within applying the ME-model, that can be seen as quality concerns when deciding the class number of blast strength. This would require specialist knowledge and experience of the system at place, as well as good knowledge on cloud dispersion throughout an area. This includes being able to define an obstructed region. (Hansen) Further, assuming the centre of explosion is often difficult due to asymmetric clouds and accounting for obstacles. In addition, as discovered in the literature review, the available experimental data for leakage is limited with special regards to larger scaled-up explosions. Also, the model does not account for inhomogeneous distribution due to non-symmetrical shape of cloud.

Guidelines has been provided by the yellow book (C. van den Bosch 2005), some methods take into account ignition strength and other apply reactivity. (Kinsella 1993), provided a table for "initial blast strength index", and three factors were defined for choosing blast strength number:

- Obstruction: High, low, none. Specified where obstacles within cloud region is more, or less than 30% of overall region fraction, or not applicable.
- Parallel plane confinement: Yes or no.
- Ignition strength: High or low.

From the number of sub explosion considered in the ME-method, several curves are presented where the positive overpressure and positive impulse which correspond to a chosen class number.

Scaled distance: $$r' = \frac{r}{(E/p_a)^{1/3}}$$ (-) (4.1)

Where r is defined as the distance from location to centre of explosion, E is available energy and p_a is the ambient pressure.

Peak overpressure: $$P_s = P_s' \cdot p_a$$ (Pa) (4.2)

Where P_s' is the scaled peak side-on overpressure, and p_a is the ambient pressure.

Positive phase duration: $$t_p = t_p' \cdot \frac{(E/p_a)^{1/3}}{a_a}$$ (s) (4.3)

Where t_p' is the scaled positive phase duration, E is available energy, p_a is the ambient pressure and a_a. Positive phase duration is defined as the period from the pressure at peak value, and the time spent decays to the when ambient pressure value is reached.

Peak dynamic pressure: $$p_{dyn} = p_{dyn'} \cdot p_a$$ (Pa) (4.4)

Where p_{dyn} is the scaled peak dynamic pressure, and p_a is the ambient pressure.

Positive impulse: $$i_s = \frac{1}{2} \cdot P_s \cdot t_p$$ (Pa•s) (4.5)

Where P_s is the side-on overpressure, and t_p is the positive phase duration.

The scaled peak values can be read of from the blast charts (P_s', p_{dyn}', t_p), see appendix E.

5.2 Hydrogen explosion study

Table 5.1 Initial conditions used for the ME method

Parameter	Notation	Value	Unit
Initial pressure	P_0	$101*10^{-3}$	Pa
Initial temperature	T_0	293	K
Molecular weight air	mw_{air}	$29*10^3$	kg/kmol
Molecular weight H_2	mw_{h2}	$2*10^3$	kg/kmol
Universal gas constant	R	8.314	kJ/kmol*K
Heat of Combustion	Q	3.5	MJ/m^3

- Determine of combustion energy.

This is calculated from the amount of explosive mass within the confined or congested area. The confined area in this case in defined as the container with one opening containing nine hydrogen cylinders. The amount of explosive mass in this area must be above the lower flammability limit for the volume to be represented.

Combustion energy = confined volume occupied by cloud * heat of combustion

- Estimate the blast strength number (1-10)

When choosing the blast strength number, this will normally require a specialist knowledge to make some subjective decisions about local circumstances. Guidelines has been provided by the yellow book (C. van den Bosch 2005), and the determination of number will be impacted by the vapour cloud ignition strength, level of obstruction and confinement. Several operators has extended the modelling for choosing strength number by using the GAME project correlation (Guidance for the Application of Multi Energy Method).

- Determine the Sachs-scaled distance

From the scaled distance variable, one can find the side-on overpressure from the blast chart, using the scaled distance and determined blast strength number. Further, calculate overpressure by using scaled distance r', and ambient pressure, p_a.

Scaled distance: $$r' = \frac{r}{(E/p_a)^{1/3}} \quad (-) \quad (4.6)$$

The overpressure is then given by:

$$p_o = r' * p_a \quad (Pa) \quad (4.7)$$

5.2.1 [1 kg] hydrogen released

The concentration of vapour in the cloud is assumed to be at stoichiometric concentrations. The cloud is confined in the container, and the nine hydrogen cylinders act as obstruction and is defined a congested area.

Class strength number chosen for all scenarios: 10.

- Cloud volume: 40m3
- Cloud centre,1: (x,y,z) (6.0, 1.3, 1.2) m. Situated middle of container.
- Cloud centre,2: (x,y,z) (12, 1.3, 1.2) m. Situated just outside the opening of container.

1. Determining charge combustion energy.

$$E = m_{h2} * Q = 40m^3 * (3.5 * 10^6)^{J}/_{m^3} = (1.4 * 10^8)J \quad (4.8)$$

where m_{h2} is mass of cloud and Q is heat of combustion.

Assuming a blast strength of x for this explosion.

2. Sachs-scaled distance.

$$r' = \frac{r}{(E/p_a)^{1/3}} = \frac{6.12m}{\frac{1.4*10^7 J}{101325 Pa}} = 0.55 \quad (4.9)$$

where r is the radius from explosion centre, E is charge combustion energy and p_a is ambient pressure.

3. Calculate overpressure with Ps' obtained from blast chart.

$$p_{o,1} = P_s' * p_a = 1.16 * 101.325\ kPa = \text{ 116kPa} \quad (4.11)$$

Figure 5.1a-b presents the obtained overpressure versus explosion distance. Figure 5.1a has the explosion centre assumed at centre of cloud (x, y, z) (6, 1.3, 1.2) m. Figure 5.1b has the explosion centre assumed at exit of hydrogen container (x, y, z) (12, 1.3, 1.2) m.

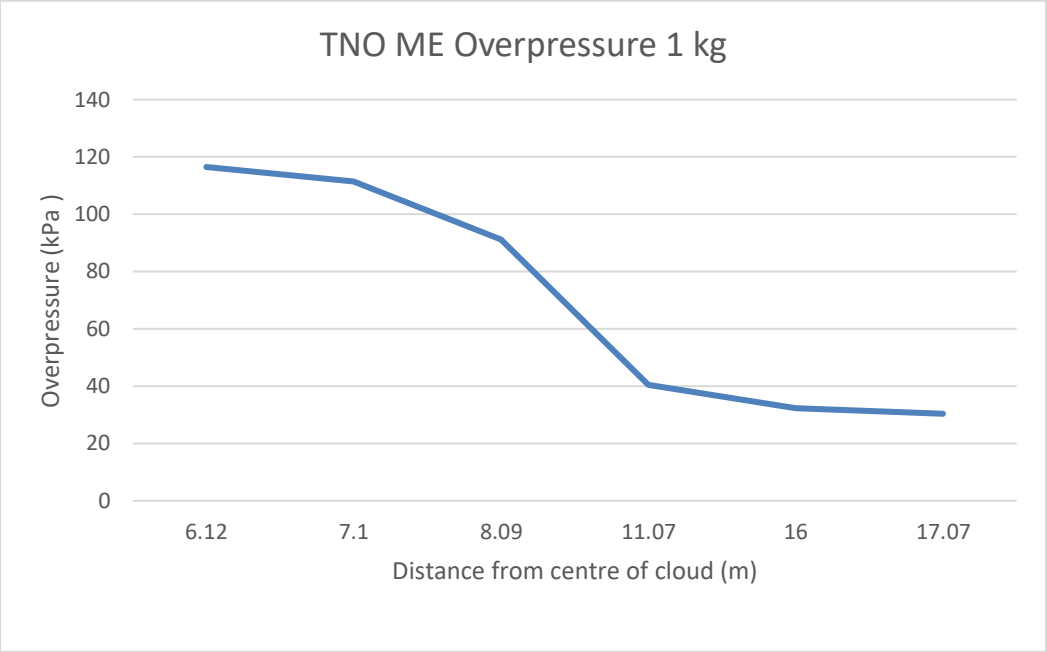

Figure 5.1a Overpressure vs. distance from centre (along x-axis towards post container).

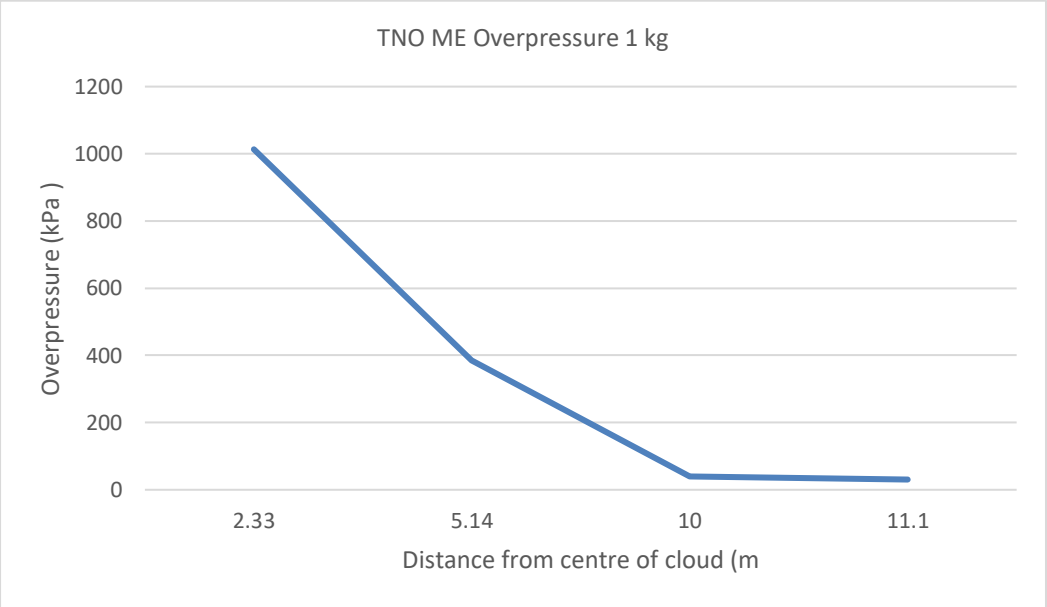

Figure 5.1b Overpressure vs. distance from centre (along x-axis towards post container).

5.2.2 [2 kg] hydrogen released

The results were split up into two separate plots to show the explosion more clearly for two different direction, x-axis and y-axis. Figure 5.2a represents the values going parallel to the contained in the x-direction, and figure 5.2b shows the values obtained across and sideways out from the container.

- Cloud volume: 80m3
- Cloud centre,1: (x,y,z) (9.0, 1.3, 1.2) m. Situated middle of container.
- Cloud centre,2: (x,y,z) (12, 1.3, 1.2) m. Situated just outside the opening of container.

1. Determining charge combustion energy.

$$E = m_{h2} * Q = 80m^3 * (3.5 * 10^6)^{J}/_{m^3} = (2.4 * 10^8)J \quad (4.10)$$

where m_{h2} is mass of cloud and Q is heat of combustion.

Figure 5.2a-b and 5.3a-b presents the obtained overpressure versus explosion distance. Figure 5.2 has the explosion centre assumed at centre of cloud (x, y, z) (9.0, 1.3, 1.2) m. Figure 5.3 has the explosion centre assumed at exit of hydrogen container (x, y, z) (12, 1.3, 1.2) m.

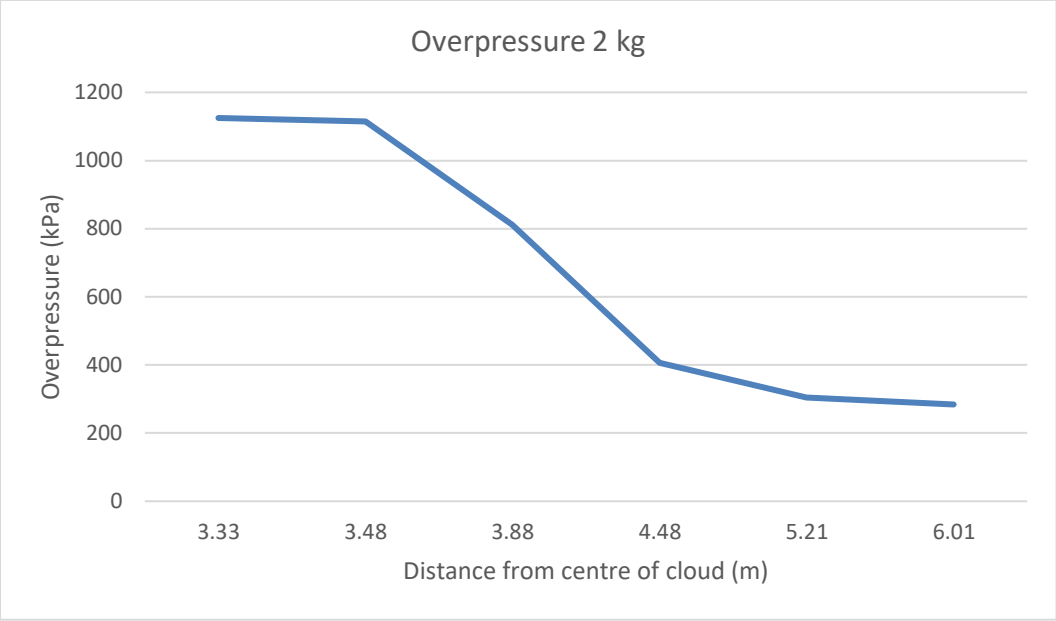

Figure 5.2a Overpressure vs. distance from centre (along x-axis towards post container).

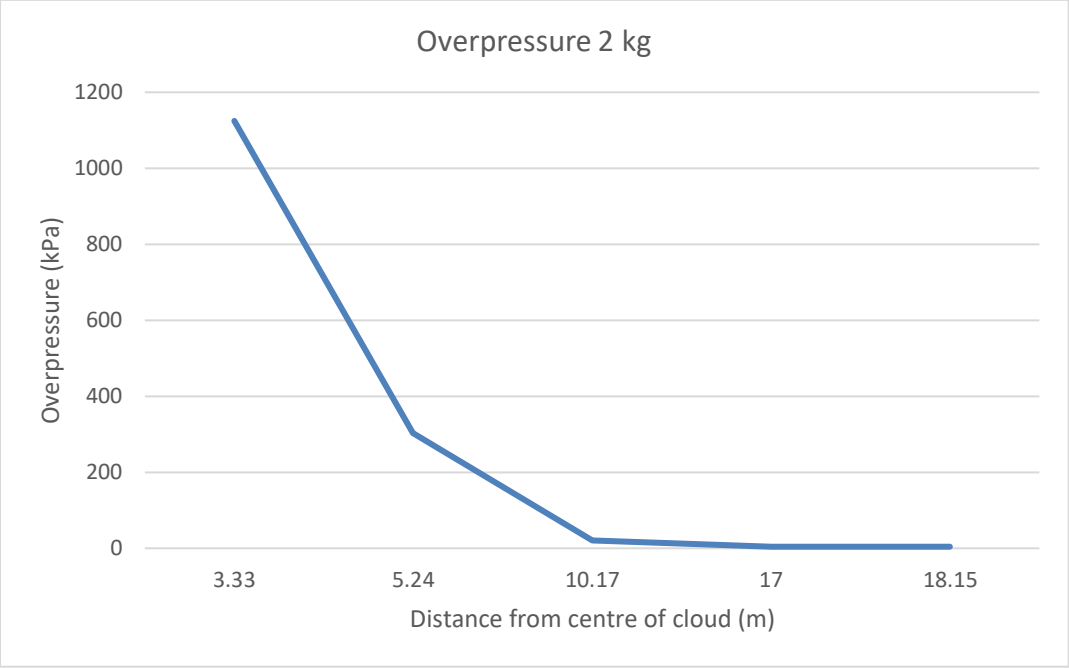

Figure 5.2b Overpressure vs. distance from centre (along y-axis on the right-hand side of container).

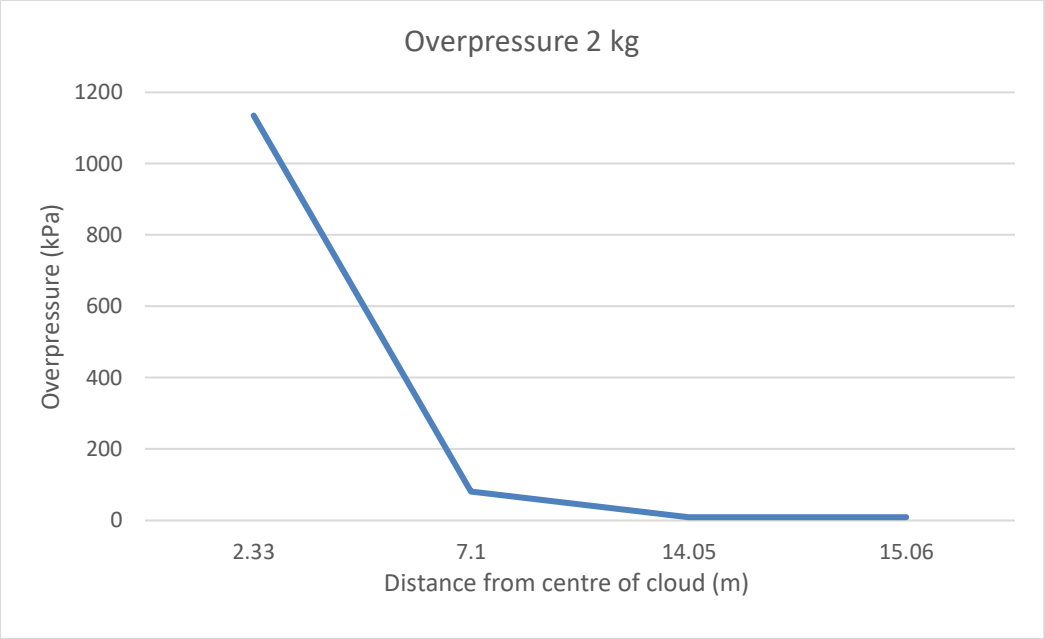

Figure 5.3a Overpressure vs. distance from centre (along x-axis towards post container).

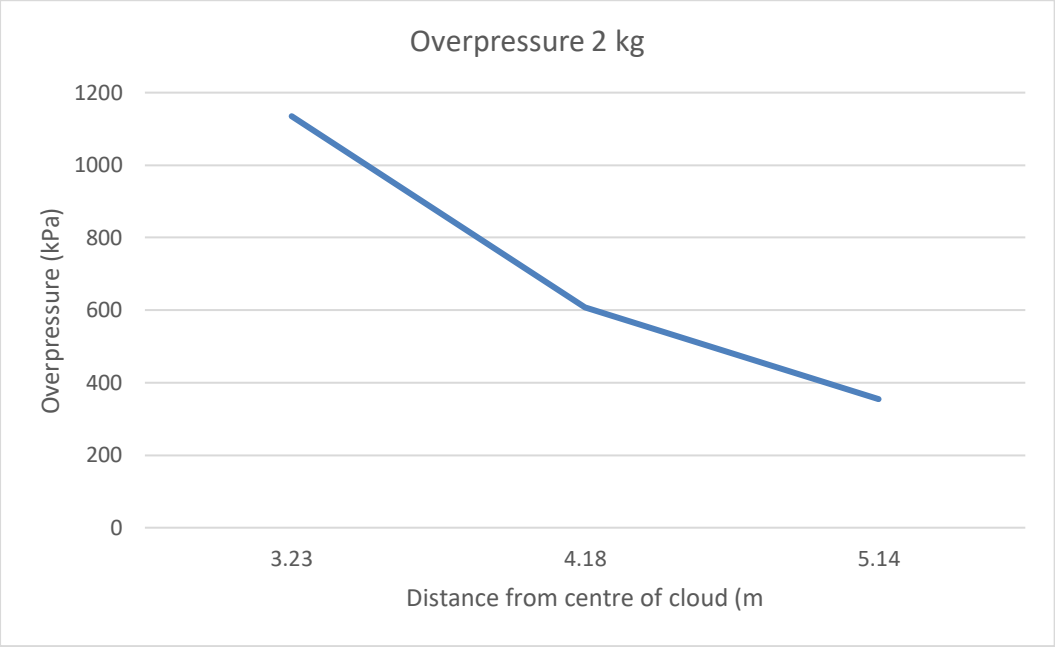

Figure 5.3b Overpressure vs. distance from centre (along y-axis on the right-hand side of container).

5.2.3 [3 kg] hydrogen released

- Cloud volume: 120m3
- Cloud centre,1: (x,y,z) (12, 1.3, 1.2) m. Situated middle of container.
- Cloud centre,2: (x,y,z) (14, 2.6, 3.2) m. Situated just outside the opening of container.

1. Determining charge combustion energy.

$$E = m_{h2} * Q = 120m^3 * (3.5 * 10^6)^{J}/_{m^3} = (4.2 * 10^8)J \quad (4.11)$$

where m_{h2} is mass of cloud and Q is heat of combustion.

Figure 5.4a-b and 5.5a-b presents the obtained overpressure versus explosion distance. Figure 5.4 has the explosion centre assumed at centre of cloud (x, y, z) (12, 1.3, 1.2) m. Figure 5.5 has the explosion centre assumed at exit of hydrogen container (x, y, z) (14, 2.6, 3.2) m.

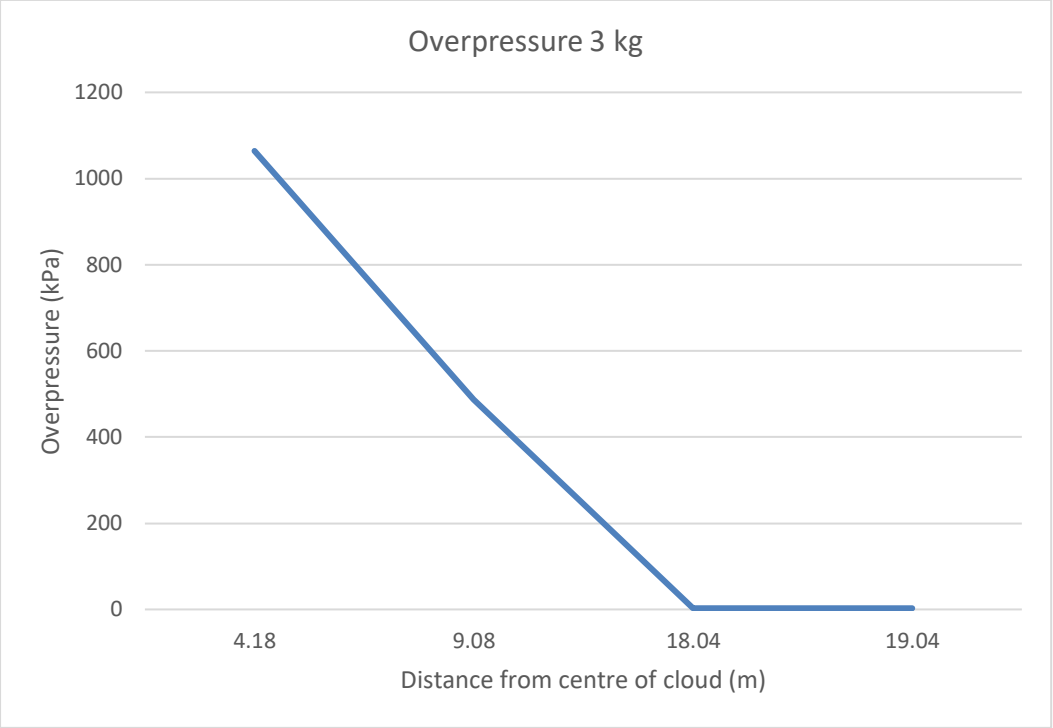

Figure 5.4a Overpressure vs. distance from centre (along x-axis towards post container).

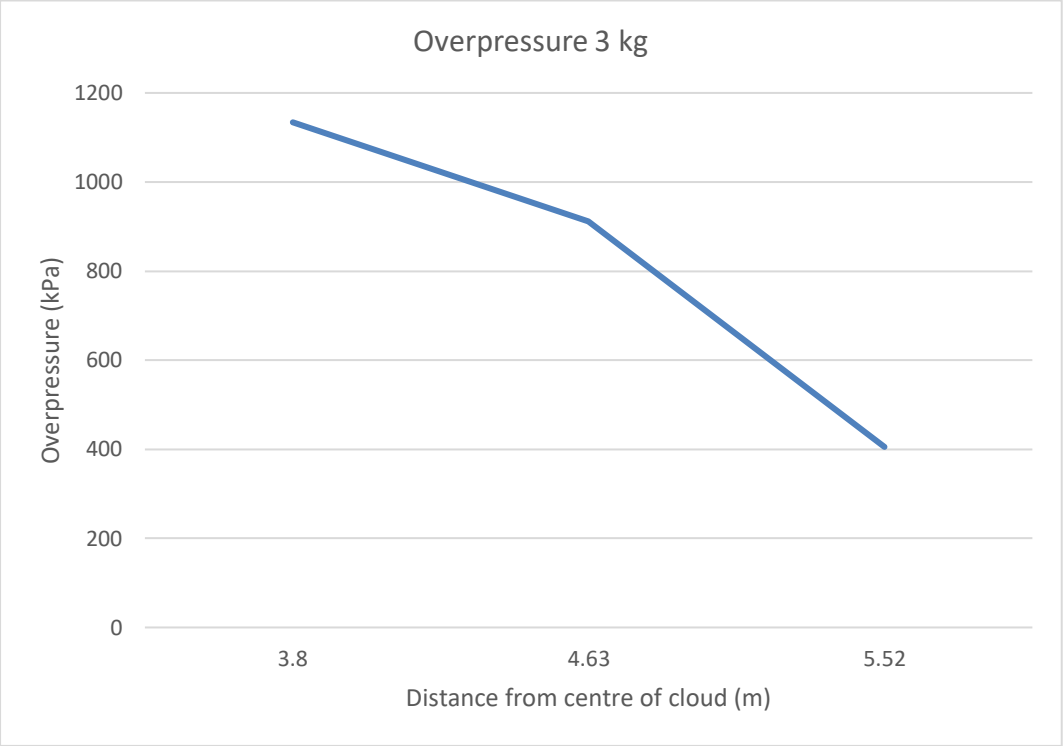

Figure 5.4b Overpressure vs. distance from centre (along y-axis on the right-hand side of container).

Centre 2

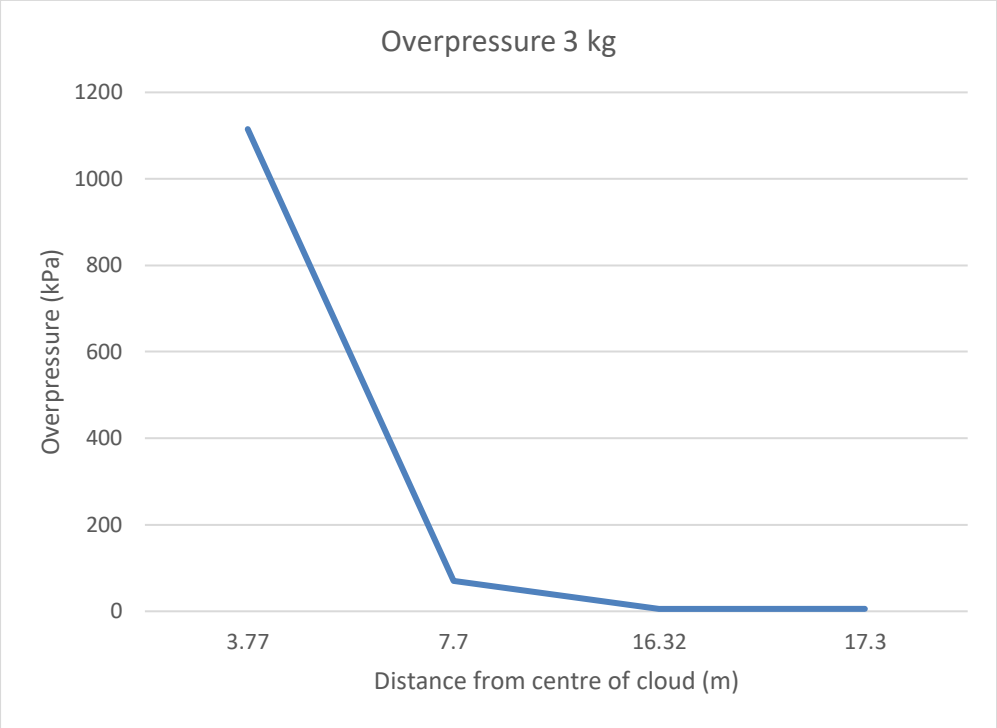

Figure 5.5a Overpressure vs. distance from centre (along x-axis towards post container).

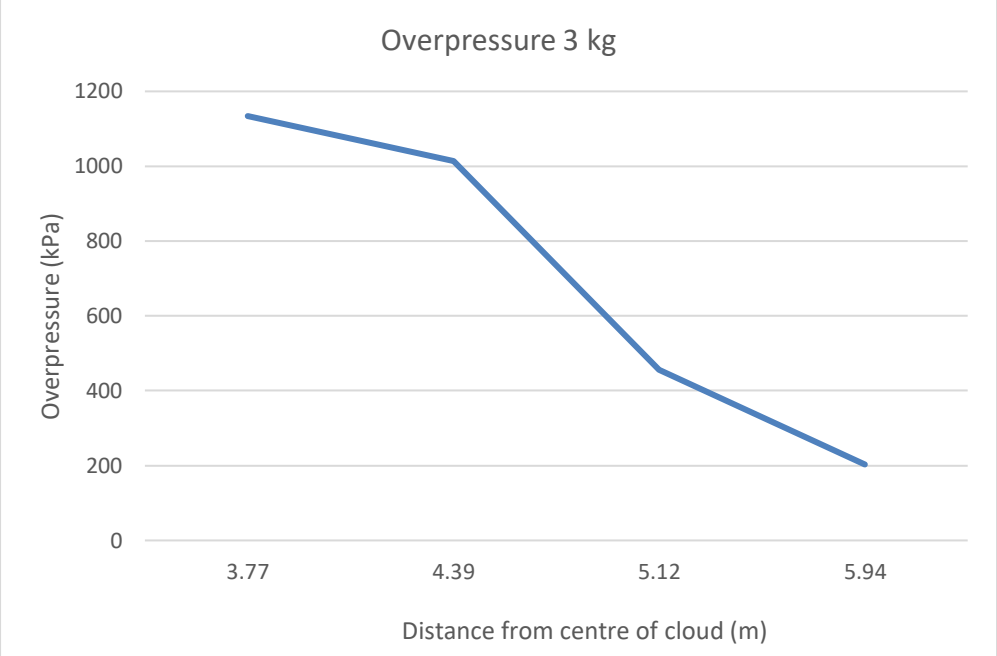

Figure 5.5b Overpressure vs. distance from centre (along y-axis on the right-hand side of container).

6 Discussion

When choosing the explosion radius (r) for calculating the Sach's scaled distance in TNO, several assumptions to the explosion behaviour was made. For 1 kg release it was assume the flame acceleration would mainly move in one direction, x. For 2kg and 3kg release the explosion was assumed to both more forward from container, as well out outwards due to 50% or more of the cloud being outside the container. The following radius were set:

- 1kg – middle of container and right outside container
- 2kg – 75% through container, and right outside container, centre of y- and z-axis.
- 3kg – Right outside container, and middle of 2nd part of cloud

For the TNO ME-model the choice of class number is left for individual discretion with limited guidance available. The class number was assumed to be 10 due to high level of obstruction in the cloud region by the container, parts or whole cloud is in parallel plane confinement covered by 3 sides. Other parameters considered was the high reactivity of hydrogen and flame speed.

In the CFD FLIC scheme the graphs show a clear detonation taking place in each scenario. Overpressure values around 20 bar was observed immediately outside the opening of the container. Figure 6.1-6.3 shows the comparison for each method for the various amount of leakage.

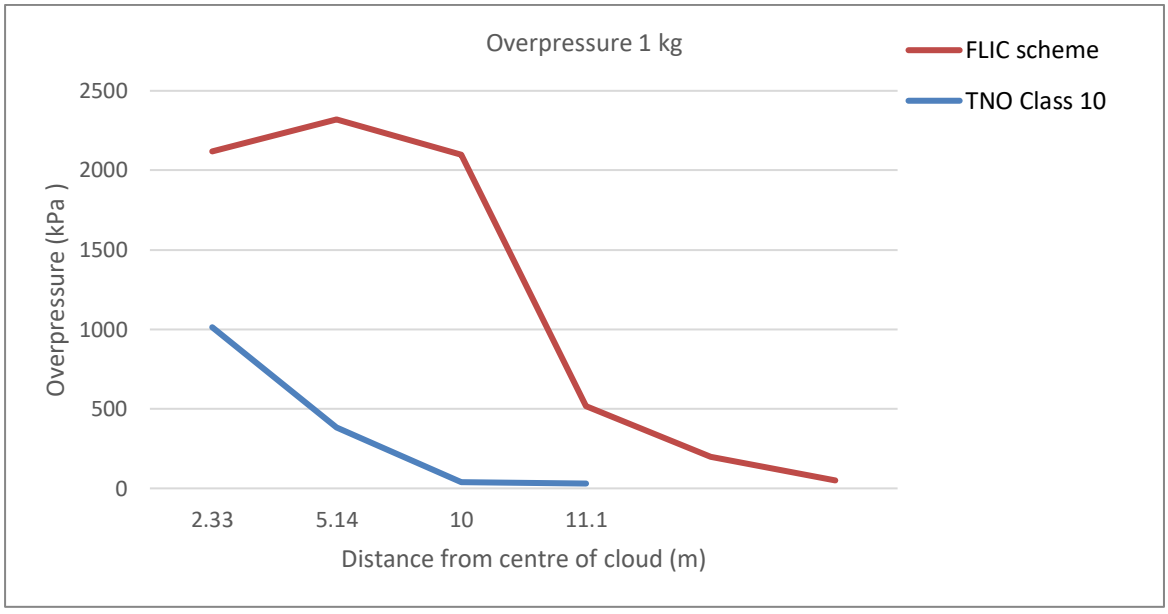

Figure 6.1 Overpressure versus explosion distance 1kg. x-direction and TNO radius outside container.

Flame acceleration for 1 kg release is assumed to act in one direction when conducting ME, which is why the sensors going outside the region on the right-hand size of container was not considered.

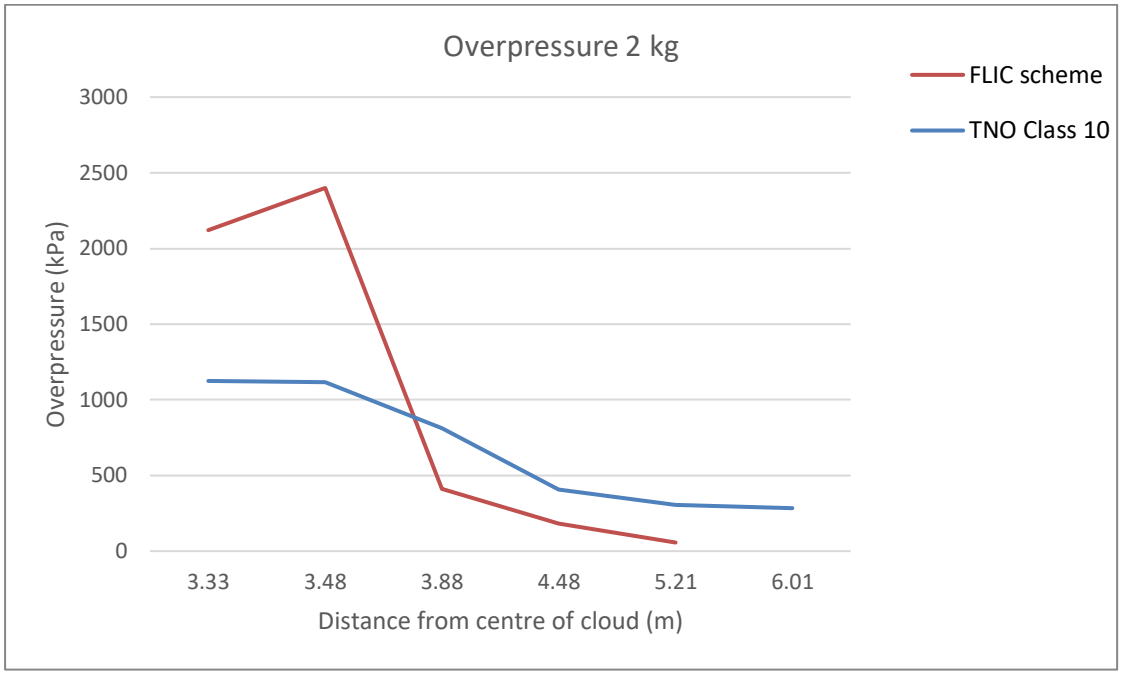

Figure 6.2 Overpressure versus explosion distance 2kg. x-direction and TNO radius placed on the outside of container.

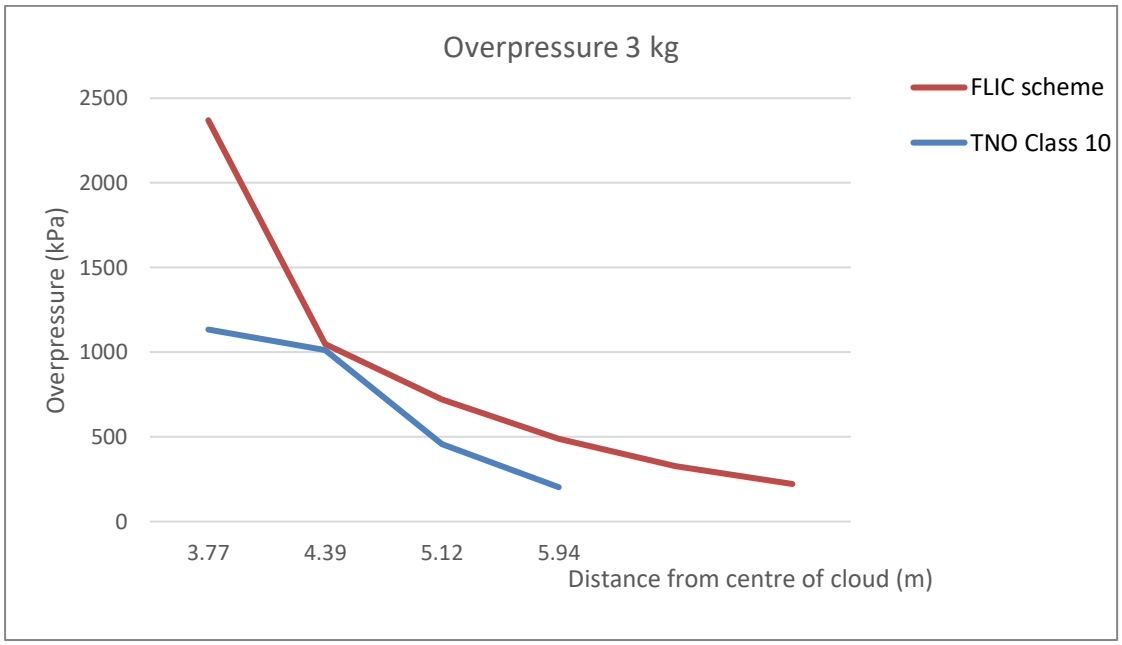

Figure 6.3 Overpressure versus explosion distance 3kg. y-direction and TNO radius in the middle of 2nd part of cloud.

The CFD and TNO returned different results for overpressure in every scenario. In Figure 6.1 the differences in the result obtained with the different methods can be explained by the calculation process of the TNO ME-method. For 1kg release, it is not able to directly include in the calculation level of confinement in the container, as well as address the cylinders in the container contributing to the blast.

Figure 6.2 shows results obtained for TNO in x-direction where radius was placed on the outside of container. The FLIC scheme returns high detonation values, but the explosion behaviour is similar for the two results. It is assumed some errors when reading of the blast chart, the scaled peak side-on overpressure, which might explain the linear “shock” obtained from TNO compared to FLIC.

Figure 6.3 presenting results obtained in the y-direction and TNO radius in the middle of 2nd part of cloud, here the best comparison result is observed. When conducting TNO the values closest to the container opening, the sensors could not be obtained as the scaled distance was too short. In consequence, the TNO model is not able to predict the immediate nearby blast seen in the FLIC scheme, but the pressure wave can be seen at 12 bars moving with similar values and CFD.

The ME-method was expected not to match the CFD results due to the geometry of the cloud, being a crescent shape moving in an upward direction, and the asymmetric shape is not possible to account for in TNO. Results show that the confined container and how obstacle geometry was placed unevenly in the cloud, is resulting is underestimating of the blast appearing outside the container. In addition, it is expected that in the CFD model there could possibly be produced excessive turbulence due to the large mesh cells size applied, which could cause an overestimation of the flame acceleration.

7 Conclusion

In this paper, the different available hydrogen storage options were investigated and reviewed. The presented work in the case study, analysed the scenario of a pre-mixed hydrogen-air vapour cloud explosion. Methods applied was the USN CFD FLIC-scheme and the TNO ME-method. These methods were later compared with regards to overpressure.

7.1 Literature review

Hydrogen has a great potential as a future fuel, but there are still many challenges to overcome in order to achieve a solid valid hydrogen economy. The storage of large amounts of hydrogen poses a hazardous risk if without proper predictions and estimations. On the contrary, because hydrogen is much lighter than air, when released it will rise and disperse into the air swiftly.

The future of hydrogen is promising. Reviewing the available literature, compressed and liquid hydrogen storage are the most developed technologies, but the volumetric density of compressed gas still requires large volume of storage and is not very effective simply because the energy density of hydrogen is quite low. Cryogenic temperature, energy density is higher, but has poor energy efficiency. Further development and construction for large-scale infrastructure is needed and more probabilistic and predictive data and simulations within this field, including production cost and leakage control. For composite and material based storage more development is necessary with regards to reliability and data showing viable long term solutions.

7.2 Case study

The comparison shows that the CFD FLIC scheme return significantly higher values for overpressure than ME-method. Differences in result for the two different methods can be explained as the ME-method was expected not to match the CFD results due to the geometry of the cloud, being a crescent shape moving in an upward direction. In addition, lower numbers might occur from the TNO ME-method not being able to calculate the level on confinement in the container, as well as address the cylinders in the container contributing to the blast.

Results obtained using CFD FLIC scheme to analyse explosion pressure gives far better results with regards to the expected behaviour of the explosion. The retrieved values simulate the occurrence of a detonation. The CFD can account for obstacles, asymmetric cloud, and other details. TNO has several limitations, and in this report the asymmetric cloud has shown to provide complications. Further, assuming the centre of explosion is often difficult due to asymmetric clouds and accounting for obstacles. TNO will better applied to a model with symmetrical cloud.

7.3 Future work

The following areas would need to be investigated for any further work on this study:

CFD model:

- Analyse bigger storage areas and higher amounts of leakage.
- Advancing scenario by adding more details and structure units.
- Refine mesh in explosion areas.

TNO ME-Method:

- Analyse higher amounts of leakage.
- More detailed analysis of blast strength number.
- Explore other values for centre of explosion
- Advance scenario by adding more details and structure units.
- Apply developed correlations to the study such as GAME.

8 References

A. Al-shanini, A. A., F. Khan (2014). "Accident modelling and safety measure design of a hydrogen station."

A. Risan, J. P. (2021). Retningslinjer for kvantitative risikovurderinger for anlegg som håndterer farlig stoff.

A. Scipioni, A. M., J. Ren (2017). Hydrogen Economy.

AIChE (2022). "Vapor Cloud Explosion (VCE)."

Alcock, J. L. (2001). "Compilation of Existing Safety Data on Hydrogen and Comparative Fuels."

Alcock, J. L. (2001). "Compilation of Existing Safety Data on Hydrogen and Comparative Fuels."

ANL (2022). "Physical Hydrogen Storage." from https://www.energy.gov/eere/fuelcells/physical-hydrogen-storage.

Australia, G. o. W. (2022). "What is a hazard and what is risk?". from https://www.dmp.wa.gov.au/Safety/What-is-a-hazard-and-what-is-4721.aspx.

B. Ehrhart, E. H. (2022). "HyRAM+." from https://energy.sandia.gov/programs/sustainable-transportation/hydrogen/hydrogen-safety-codes-and-standards/hyram/.

B. Park, e. a. (2021). "Numerical and experimental analysis of jet release and jet flame length for qualitative risk analysis at hydrogen refueling station ".

Bayes, T. (2022). "Bayesian analysis."

Berg, v. d. (1985). "The multi-energy method: A framework for vapour cloud explosion blast prediction."

C. C. Jullian, K. M. G. (2021). "Data requirements for improving the Quantitative Risk Assessment of liquid hydrogen storage systems."

C. Jullian , K. M. G. (2022). "Data requirements for improving the Quantitative Risk Assessment of liquid hydrogen storage systems."

C. van den Bosch, R. W. (2005). Methods for the calculation of physical effects 'yellow book'.

EIA (2016). "Hydrogen for refineries is increasingly provided by industrial suppliers." from Hydrogen for refineries is increasingly provided by industrial suppliers.

Energy (2022). "Liquid Hydrogen Delivery." from https://www.energy.gov/eere/fuelcells/liquid-hydrogen-delivery.

Energy, O. o. E. E. a. R. (2022) Hydrogen Fuel Basics.

Energy, U. D. o. (2022). "Sorbent Storage Materials." from https://www.energy.gov/eere/fuelcells/sorbent-storage-materials.

Engie (2021). "H2 in the underground: Are salt caverns the future of hydrogen storage?". from https://innovation.engie.com/en/articles/detail/hydrogen-underground-storage-salt-caverns/25906/general.

F. Rigas, S. S. (2005). "Evaluation of hazards associated with hydrogen storage facilities."

Frost, J. (2022). "Weibull Distribution: Uses, Parameters & Examples."

Geel, v. (2005). Guidelines for quantitative risk assessment.

Ghafri, S. A. (2022). "Modelling of Liquid Hydrogen Boil-Off."

Gkanas, E. (2020). Introduction on Hydrogen Storage.
,
FCH2edu.

Global, T. (2022). "WHAT IS HYDROGEN STORAGE AND HOW DOES IT WORK?". from https://www.twi-global.com/technical-knowledge/faqs/what-is-hydrogen-storage.

Gunawan, P. (2018). "Simulation of shoreline development in a groyne system, with a case study Sanur Bali beach."

H. Dagdougui, e. A. (2018). "Hydrogen Logistics: Safety and Risks Issues."

H. Versteeg, W. M. (2007). An Introduction to Computational Fluid Dynamics.

H.Wilkening, D. B. (2007). "CFD modelling of accidental hydrogen release from pipelines."

Hansen, O. R. Using CFD for Blast Wave Predictions.

Hansen, O. R. (2019). "Hydrogen Infrastructure - Efficient Risk Assessment and Design Optimization Approach."

Hansen, O. R. (2019). "Hydrogen Safety: Kjørbo-incident, overview and perspectives."

Hereon (2022). "Overview: Hydrogen." from https://hereon.de/about_us/overview/hydrogen/index.php.en.

IEA (2019). "The Future of Hydrogen."

J Anderson, S. G. (2019). "Large-scale storage of hydrogen."

J. Dunjo, M. A., N. Prophet (2017). "An Overview of Quantitative Risk Assessment Methodology, and Worldwide Risk Tolerability Criteria." from https://www.mepsc.org/?display_media=1861.

Jiang, Z. (2022). "Feasibility Invetigation of Several Hydrogen Generation & Storage Methods."

K. Shaba, C. H. (2022). "Why frequency analysis in QRAs?".

Karanam, e. A. (2021). "TimeScale Analysis, Numerical Simulation and Validation of Flame Acceleration, and DDT in Hydrogen-Air Mixtures."

Kinsella (1993). "A rapid assessment methodology for the prdiction of vapour cloud explosion overpressure."

L. Melani, e. a. (2007). "Review methods estimating overpressure and impulse resulting hydrogen explosion."

LaChance, e. a. (2009). Analyses to support development of risk-informed separation distances for hydrogen codes and standards.

M. Kodoth, e. A. (2020). "Leak frequency analysis for hydrogen-based technology using bayesian and frequentist methods."

Mathworks (2022). MatLAB.

Nichols, R. (2003). Turbulence Models In CFD.

Panel, H. S. (2021). Report on the June 2019 Hydrogen Explosion and Fire Incident in Santa Clara, California.

Purewal, J. (2010). Hydrogen Adsorption by Alkali Metal Graphite Intercalation Compounds.

R. Moradi, K. M. G. (2019). "Hydrogen storage and delivery: Review of the state of the art technologies and risk and reliability."

Rosyid, A. (2006). "System-analytic Safety Evaluation of the Hydrogen Cycle for Energetic Utilization."

S. Hanna, P. D. (1987). Guidelines for use of vapour cloud dispersion models

Sandia (2022). "HyRAM." from https://energy.sandia.gov/programs/sustainable-transportation/hydrogen/hydrogen-safety-codes-and-standards/hyram/.

Shell (2022) Hydrogen.

Smith, D. J. (2005). Reliability, Maintainability and Risk (Seventh Edition).

T. Smolinka, J. G. (2021). Electrochemical Power Sources: Fundamentals, Systems, and Applications.

Toro, E. F. (2009). Riemann Solvers and Numerical Methods for Fluid Dynamics.

Tretsiakova-McNally, S. (2022). Dealing with hydrogen explosions.

Vågsæther, K. (2010). "Modelling of gas explosions."

W. Yuan, e. a. (2022). "Numerical investigation of the leakage and explosion scenarios in China's first liquid hydrogen refueling station."

Zeng, X. (2022). "High-Resolution Finite Volume Methods." from https://www.math.utep.edu/faculty/xzeng/2021spring_math5343/files ln09_highres.pdf.

Zipf, R. (2022). Effects of blast pressure on structures and the human body.

9 Appendices

Appendix A: Topic description

FMH606 Master's Thesis

Title: Risk assessment methodology for large hydrogen systems
USN supervisor: Knut Vågsæther
External partner: N/A

Task background:
For handling larger amounts of hydrogen, Quantitative Risk Assessment (QRA) is often required. A QRA will determine safety distances for a system based on risk. There is no way of knowing if the predicted risk for a system is correct, but a structured analysis of the methodology and use of existing experimental results might help in understanding and possibly estimate uncertainties in the calculations. Accidents, like the incident at Kjørbo[1], and large-scale experiments from several research projects can be used together with risk and consequence tools to perform the analysis (HyRAM[2]).

Task description:

- Literature review on QRA and consequence prediction methods for hydrogen
- Use CFD code to simulate explosion pressure and distance
- Compare CFD simulation results with calculations using TNO Multi Energy method.

Student category: EET, PT
Is the task suitable for online students (not present at the campus)? Yes

Practical arrangements:
Possibly use an in-house CFD code for explosions to study important effects that comes up in study. The research group of Process safety, combustion and explosions is arranging the international conference ISFEH10 in May 2022 (isfeh10.org), students may be part of the organizing team during the conference.

Supervision:
As a general rule, the student is entitled to 15-20 hours of supervision. This includes necessary time for the supervisor to prepare for supervision meetings (reading material to be discussed, etc).

Signatures:
Supervisor (date and signature): KNUT VÅGSÆTHER
Student (write clearly in all capitalized letters): CATHRINE VINDENES
Student (date and signature): CV

Appendix B: The Algorithm (Flowchart) of the Original USN-FLIC Code

Appendix C: Initial Conditions MatLAB (IC.m)

```
function
[r,p,ux,uy,uz,g,alpha,beta,k,f,gaunburn,gaburn,gaair,mw,mwb,Q,imax,dx,dy,dz,n,h,bz
,tmax,en,pb,Cs,Cfl,se,ign,XS,YS,ZS,PS,sav,K,Rx]=IC(C);
if C==1;
    % Domain, cell number n=x, h=y, bz=z
    n=420;
    h=125;
    bz=80;

    % Max number of time steps
    imax=1500;
    % Cell sizes
    dx=10e-2;                   %0.1m
    dy=10e-2;
    dz=10e-2;
    % Initial states
    mw=29e-3;                   %Reactants
    mwb=29e-3;                  %Burnt
    p0=1e5;                     %Initial pressure
    u1=0;                       %Initial speed
    T0=293;                     %Initial temperature
    r0=1.2;                     %Density

    g1=1.4;                     %Heat capacity ratio
    gaunburn=1.4;               %Heat capacity ratio

    gaburn=1.4;                 %Heat capacity ratio
    gaair=1.4;                  %Heat capacity ratio
    Q(1:n,1:h,1:bz) = 3.5e6;    %Heat of combustion
    q=max(max(Q));
    p(1:n,1:h,1:bz)=p0;

    r(1:n,1:h,1:bz)=r0;
    ux(1:n,1:h,1:bz)=0;
    uy(1:n,1:h,1:bz)=0;
    uz(1:n,1:h,1:bz)=0;
    k(1:n,1:h,1:bz)=0;
    g(1:n,1:h,1:bz)=g1;
    alpha(1:n,1:h,1:bz)=0;
    beta(1:n,1:h,1:bz)=1;       %Reaction variable, 1=not reacted
    f(1:n,1:h,1:bz)=0;          %f is transported with the cloud,1=reactive

    % Set initial hydrogen cloud
    f(1:120,50:76,1:25)=1;      %Gas present, shape of cloud
    r(1:120,50:76,1:25)=0.97;   %Cloud density

    % add one kg of H2
    f(121:160,50:76,13:52)=1;
    r(121:160,50:76,13:52)=0.97;

    % add one kg of H2
    f(161:200,50:76,33:72)=1;
    r(161:200,50:76,33:72)=0.97;
```

```
% Ignition point
    beta(1:2,51:53,1:2)=0;      %Reaction variable
    nkn=find(beta==0);
    r(nkn)=0.08;

    ign=nkn;

    % Set pressure sensor positions
    XS=[141,141,141,141,141,141,161,210,300,310];
    YS=[63,53,43,33,23,13,63,63,63,63];
    ZS=[1,1,1,1,1,1,1,1,12,27];
    for j=1:length(XS);
        PS(j)=p(XS(j),YS(j),ZS(j));
    end
    % Set how often (time step) to store pressure and density field
    sav=100;

    % Max simulation time
    tmax=10;

    Rx=1;   % Rx=1 is a course mesh reaction rate,
            % Rx=0 is a more detailed rate that needs finer mesh (<= 1 mm).

    nd=0;

    K=1;    % A factor multiplied with the modelled turbulent burning velocity,
            % by setting above 1 flame is pushed towards kineticcontolled rate
    en=0;
    se=1;
    syl=0;
    pb=0;
    Cs=0.067;
    Cfl=0.9;

end
```

Appendix D: Geometry MatLAB

```
function [lx,ly,lz,hx,hy,hz,fill]=Geometry(n2,h,b,n);
if n==1
    s(1:n2,1:h,1:b)=0;
    % Define geometry (s(x,y,z)=1 means solid)
    s(1:120,50,1:25)=1;
    s(1:120,76,1:25)=1;
    s(1:120,50:76,26)=1;

    Y=[55,55,55,63,63,63,71,71,71];
    Z=[4,12,20,4,12,20,4,12,20];
    r=3;
    L=120;
    for i=1:length(Y);
        s=Cylinder_x(s,1,Y(i),Z(i),r,L); % Cylinder geometry
    end
    s(1,50:76,1:25)=1;
    s(301:end,50:76,1:25)=1;

end

slx=[s(1,:,:);s(1:n2-1,:,:)];
lx=find(slx>s);
shx=[s(2:n2,:,:);s(n2,:,:)];
hx=find(shx>s);
sly=[s(:,1,:),s(:,1:h-1,:)];
ly=find(sly>s);
shy=[s(:,2:h,:),s(:,h,:)];
hy=find(shy>s);
slz=cat(3,s(:,:,1),s(:,:,1:b-1));
lz=find(slz>s);
shz=cat(3,s(:,:,2:b),s(:,:,b));
hz=find(shz>s);
fill=find(s==1);
```

Appendix E: TNO Multi Energy Method BLAST charts

Figure 1: Multi Energy method blast chart: Peak side-on overpressure

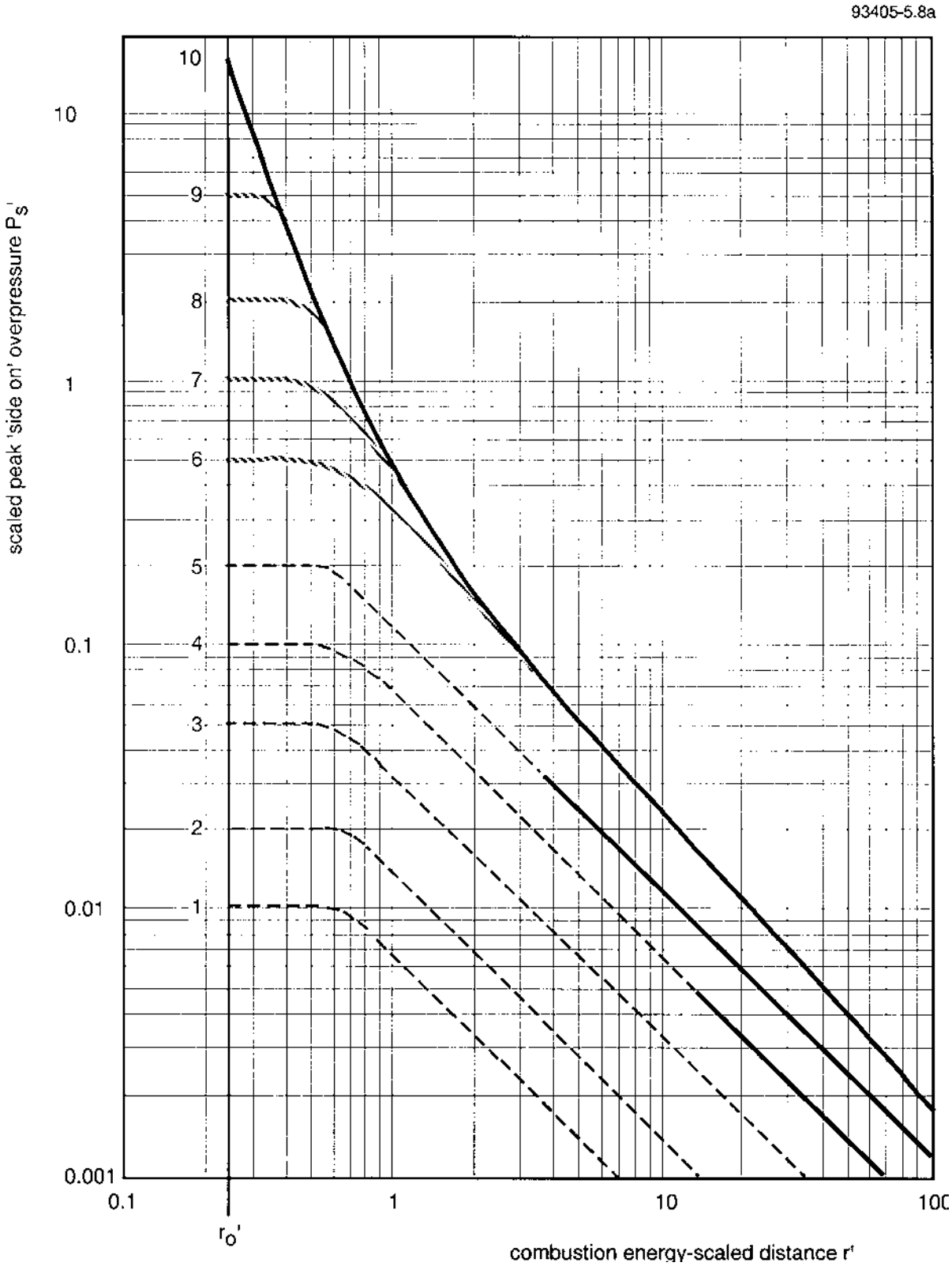

Figure 2: Multi Energy method blast chart: Peak dynamic pressure

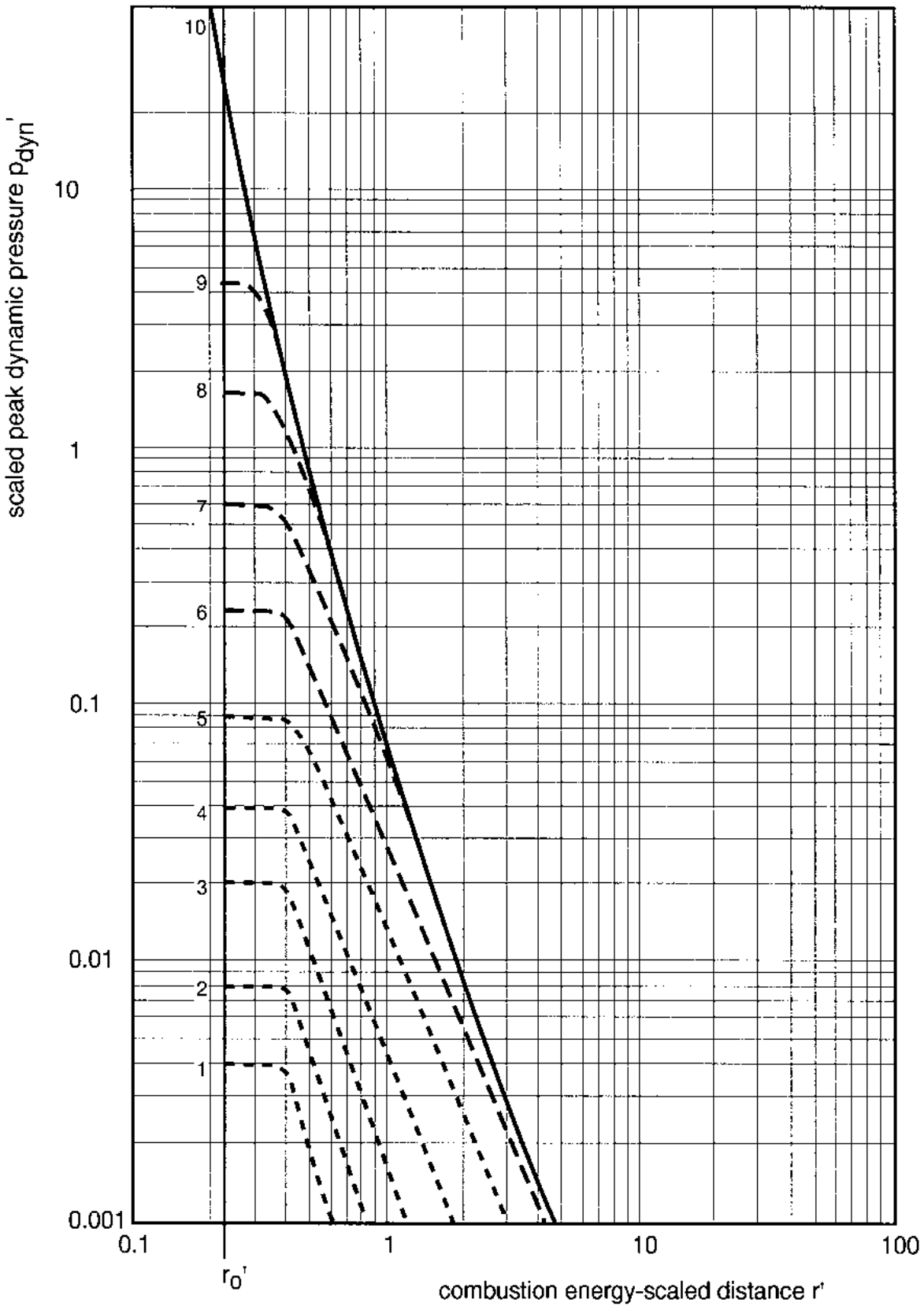

Figure 3: Multi Energy method blast chart: Positive phase duration and blast-wave shape

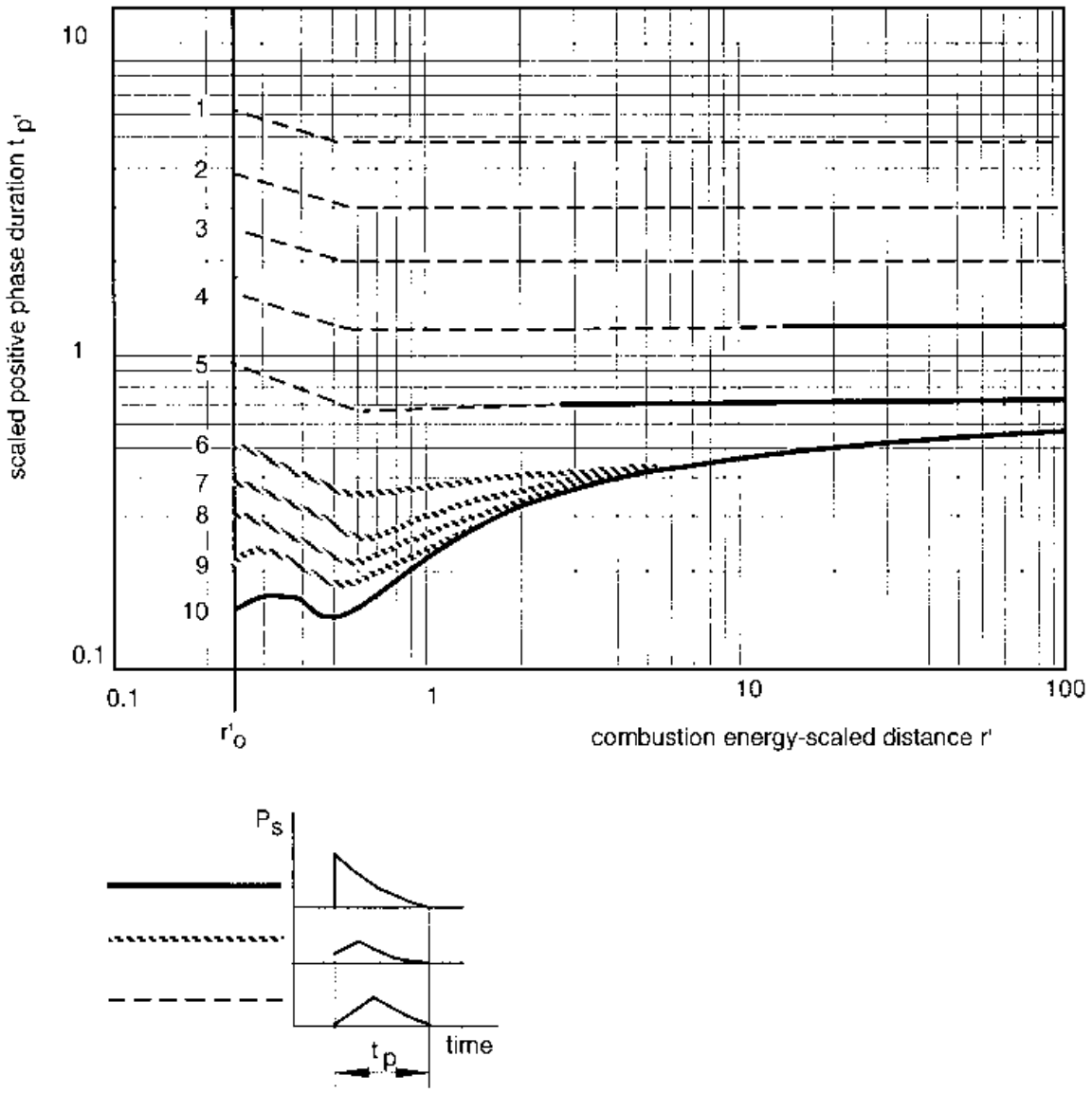

Appendix F: TNO Multi Energy Flow Diagram

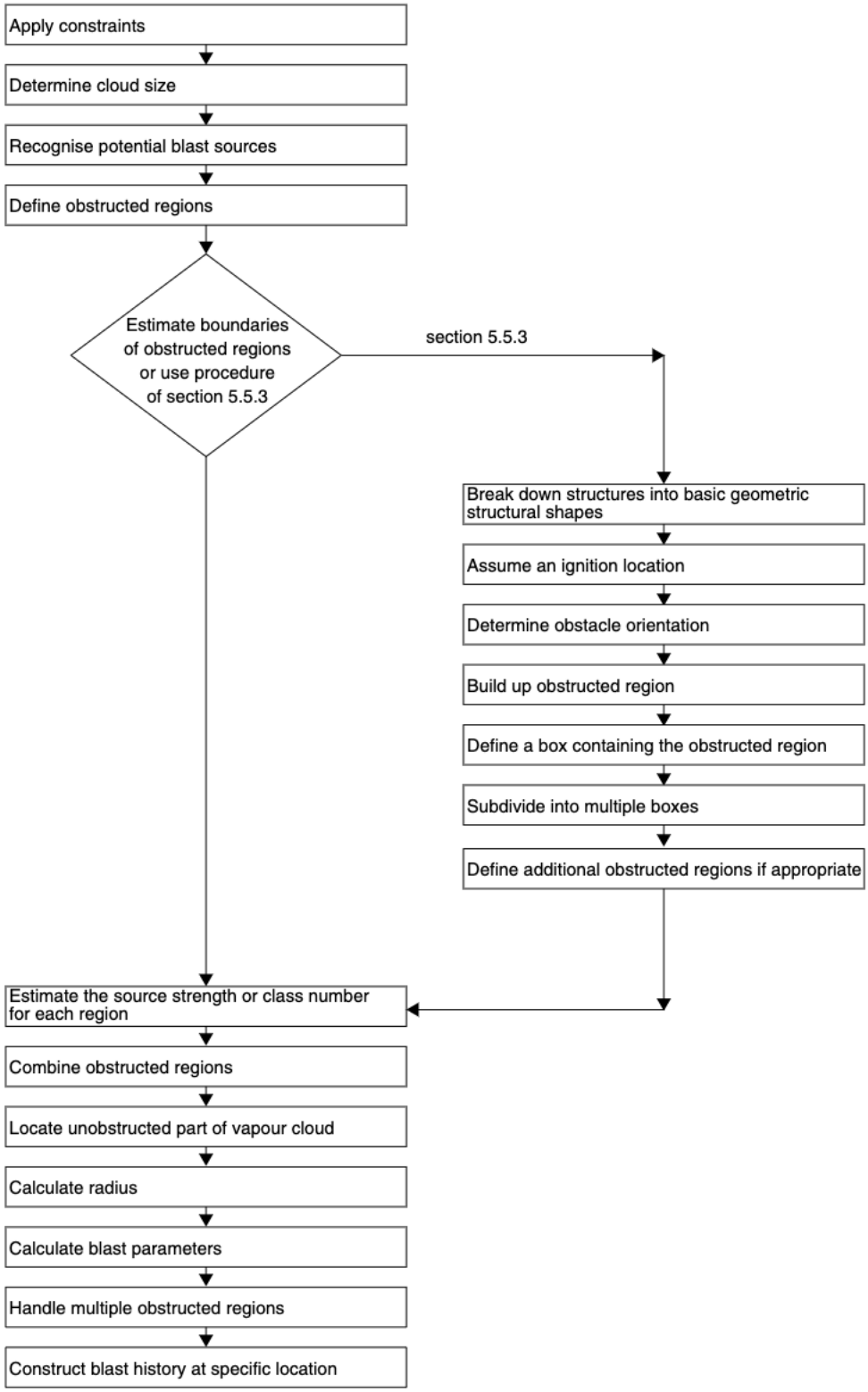

Figure 5.9 Flow diagram for application of the method